[UCI]I804:24011-200000233892

2007 년 2 월

박사학위논문

THE EFFECT OF QUERCETIN AND (-)-EPIGALLOCATECHIN GALLATE ON THE BIOAVAILABILITY OF ETOPOSIDE IN RATS

조선대학교 대학원

약학과

이 수 국

THE EFFECT OF QUERCETIN AND (-)-EPIGALLOCATECHIN GALLATE ON THE BIOAVAILABILITY OF ETOPOSIDE IN RATS

흰쥐에서 퀠세틴과 카테친이 에토포시드의 생체이용율에 미치는 영향

2007 년 2 월 25 일

조선대학교 대학원

약학과

이 수 국

THE EFFECT OF QUERCETIN AND (-)-EPIGALLOCATECHIN GALLATE ON THE BIOAVAILABILITY OF ETOPOSIDE IN RATS

지도교수 최 준 식

이 논문을 약학박사학위신청 논문으로 제출함.

2006 년 10 월

조선대학교 대학원

약학과

이 수 국

이수국의 박사학위논문을 인준함

위원장	서울대학교	교수	이명걸	인
위 원	전남대학교	교수	신상철	인
위 원	조선대학교	교수	최후균	인
위 원	조선대학교	교수	한효경	인
위 원	조선대학교	교수	최준식	인

2006 년 12 월

조선대학교 대학원

Contents

ABSTRACT……1

국문초록……4

1. INTRODUCTION……8

2. MATERIALS AND METHODS……21

2.1. Materials……21

2.2. HPLC analysis……21

2.2.1. Instrumentation……21

2.2.2. Chromatographic conditions……21

2.2.3. Preparation of stock solutions ……22

2.2.4. Preparation of analytical standard solutions …… 22

2.2.5. Sample preparation……22

2.2.6. Validation procedures……22

2.2.6.1. Linearity ……23

2.2.6.2. Recovery……23

2.2.6.3. Intra– and inter–day variability……23

2.3. Animal experiments……24

2.4. Drug administration and sampe collection ……24

2.4.1. Intravenous (i.v.) administration of etoposide ……25

2.4.2. Intraportal (i.p.) administration of etoposide ……25

2.4.3. Intragastric (i.g.) administration of etoposide ……25

2.4.4. Preadministration of verapamil……25

2.4.5. Preadministration of quercetin……26

2.4.6. Preadministration of EGCG……26

2.5. Pharmacokinetic analysis……26
2.6. Statistical analysis……27
3. RESULTS……28
3.1. Chromatographic separation……28
3.2. Validation characteristics of analysis ……28
3.3. Pharmacokinetics of etoposide in rats after i.v., i.p. and i.g. administration……29
3.4. Effect of verapamil on the pharmacokinetics of etoposide……29
3.5. Effect of quercetin on the pharmacokinetics of etoposide……30
3.6. Effect of EGCG on the pharmacokinetics of etoposide……31
4. DISCUSSION……33
5. CONCLUSION……40
REFERENCES……42

List of Tables

Table 1. Recovery of etoposide and podophyllotoxin from rat's plasma…56

Table 2. Precision and accuracy of HPLC assay for etoposide from rat plasma……57

Table 3. Mean (+ S.D.) plasma concentration of etoposide after administration of etoposide through intravenous (3.3 mg/kg), intraportal (3.3 mg/kg) and intragastric (10 mg/kg) routes in rats (n = 6, respectively). ……58

Table 4. Mean (+S.D.) plasma concentration of etoposide after intravenous administration at a dose of 3.3 mg/kg in the presence or absence of verapamil at the dose of 2 or 6 mg/kg in rats (n = 6, respectively). … … … … … … … 59

Table 5. Mean (+ S.D.) plasma concentration of etoposide after intragastric administration at a dose of 10 mg/kg in the presence or absence of verapamil at doses of 2 or 6 mg/kg to rats (n = 6, respectively).……60

Table 6. Mean (+ S.D.) plasma concentration of etoposide after intravenous administration of etoposide at a dose of 3.3 mg/kg in the presence or absence of quercetin at doses of 3, 12 or 20 mg/kg to rats (n = 6, respectively).…61

Table 7. Mean (+ S.D.) plasma concentration of etoposide after intragastric administration of etoposide at a dose of 10 mg/kg in the presence or absence of quercetin at the dose of 3, 12 or 20 mg/kg to rats (n = 6, respectively).62

Table 8. Mean (+S.D.) plasma concentration of etoposide after intravenous administration of etoposide at a dose of 3.3 mg/kg in the presence or absence of EGCG at doses of 3 and 12 mg/kg to rats (n = 6, respectively).……63

Table 9. Mean (+ S.D.) plasma concentration of etoposide after intragastric administration at a dose of 10 mg/kg in the presence or absence of EGCG at doses of 3, 12 or 20 mg/kg to rats (n = 6, respectively).……64

Table 10. Mean (+ S.D.) pharmacokinetic parameters of etoposide after intravenous administration of etoposide at a dose of 3.3 mg/kg in the presence or absence of verapamil at doses of 2 and 6 mg/kg to rats (n = 6, respectively).·····65

Table 11. Mean (+ S.D.) pharmacokinetic parameters of etoposide after intragastric administration of etoposide at a dose of 10 mg/kg in the presence or absence of verapamil at doses of 2 and 6 mg/kg to rats (n = 6, respectively).·····66

Table 12. Mean (+ S.D.) pharmacokinetic parameters of etoposide after intravenous administration of etoposide at a dose of 3.3 mg/kg in the presence or absence of quercetin at doses of 3, 12 or 20 mg/kg to rats (n = 6, respectively). ···67

Table 13. Mean (+ S.D.) pharmacokinetic parameters of etoposide after intragastric administration of etoposide at a dose of 10 mg/kg in the presence or absence of quercetin at doses of 3, 12 or 20 mg/kg to rats (n = 6, respectively). ···68

Table 14. Mean (+ S.D.) pharmacokinetic parameters of etoposide after intravenous administration of etoposide at a dose of 3.3 mg/kg in the presence or absence of EGCG at doses of 3 and 12 mg/kg to rats (n = 6, respectively). ·····69

Table 15. Mean (+ S.D.) pharmacokinetic parameters of etoposide after intragastric administration of etoposide at a dose of 10 mg/kg in the presence or absence of EGCG at doses of 3, 12 or 20 mg/kg to rats (n = 6, respectively). ·····70

List of Figures

Figure 1. Transmembrane arrangement of ABC efflux proteins. ……71

Figure 2. Chemical structure of trans-lactone (A) of etoposide and its degraded pharmacologically inactive isomer cis-lactone form (B) which produced in neutral, weak acidic and alkaline conditions, and the phase I metabolite, etoposide catechol (C). … … … … … … … … … … … … … … … … … … … 72

Figure 3. The chemical structure of flavonoids based on a C_{15} skeleton can be represented as the C_6- C_3 - C_6 system (A). A CHROMANE ring bearing a second aromatic ring B in position 2, 3 or 4 (B). ……73

Figure 4. Major subgroups of flavonoids. ……74

Figure 5. Biotransformation scheme of the nature quercetin (glucosides) via gastrointestinal system. (Structures of quercetin, isoquercitrin and rutin, and the methylated quercetin metabolites, isorhamnetin and tamarixetin). ……75

Figure 6. Chemical structures of catechins. ……76

Figure 7. Chromatogram of blank rat plsma (A) and the plasma after oral adminstration of verapamil without etoposide adminstration (B, verapamil retention time 2.4 min), and the plasma 2h after i.g. administration of etoposide at a dose of 10 mg/kg (C, podophyllotoxin at 5.4 min and etoposide at 11.1 min). … 77

Figure 8. Calibration curve of etoposide when spiked in rat's blank plasma. ……78

Figure 9. Mean plasma concentration-time profiles of etoposide after intravenous (3.3 mg/kg), intraportal (3.3 mg/kg) and intragastric (10 mg/kg), administration of etoposide to rats (n = 6, respectively).……79

Figure 10. Mean dose-normalized (based on the dose of 3.3 mg/kg) AUC values of etoposide following intravenous and intraportal administration at the dose of 3.3 mg/kg and intragastric administration at a dose of 10 mg/kg to rats (n = 6, respectively). …… 80

Figure 11. Mean plasma concentration-time profiles of etoposide after intravenous administration of etoposide at a dose of 3.3 mg/kg to rats in the presence or absence of verapamil at doses of 2 and 6 mg/kg (n = 6, respectively). …… 81

Figure 12. Mean plasma concentration-time profiles of etoposide after intragastric administration of etoposide at a dose of 10 mg/kg to rats in the presence or absence of verapamil at doses of 2 and 6 mg/kg (n = 6, respectively). …… 82

Figure 13. Mean plasma concentration-time profiles of etoposide after intravenous administration of etoposide at a dose of 3.3 mg/kg to rats in the presence or absence of quercetin at doses of 3, 12 and 20 mg/kg (n = 6, respectively). …… 83

Figure 14. Mean plasma concentration-time curves of etoposide after oral administration of etoposide at a dose of 10 mg/kg to rats in the presence or absence of quercetin at doses of 3, 12 and 20 mg/kg (n = 6, respectively). …… 84

Figure 15. Mean plasma concentration-time profiles of etoposide after intravenous administration of etoposide at a dose of 3.3 mg/kg to rats in the presence or absence of EGCG at doses of 3 and 12 mg/kg (n = 6, respectively). …… 85

Figure 16. Mean plasma concentration-time curves of etoposide after intragastric administration of etoposide at a dose of 10 mg/kg to rats in the presence or absence of EGCG at doses of 3, 12 and 20 mg/kg (n = 6, respectively). 86

Figure 17. Efflux transporters and intracellular metabolic enzymes in intestinal epithelia (A) and hepatocytes (B) ……87

ABSTRACT

THE EFFECT OF QUERCETIN AND (-)-EPIGALLOCATECHIN GALLATE ON THE BIOAVAILABILITY OF ETOPOSIDE IN RATS

Xiuguo Li
Advisor: Prof. Jun-Shik Choi, Ph.D.
Department of Pharmacy,
Graduate School of Chosun University

Transporters-based multidrug resistance (MDR) is a main barrier for many anticancer agents to gain a successful chemotherapy. The oral bioavailabilitiy of many anticancer agents are low which contribute highly to the first-pass extraction caused mainly by phase I and phase II metabolism and the members of ATP-binding cassette (ABC) superfamily mediated efflux in the intestine and liver. Orally administered etoposide is a substrate for efflux of ABC transporters and the phase I and phase II metabolizing enzymes, specifically P-gp and CYP3A. This study investigated the pharmacokinetics of etoposide after administration through intravenous (i.v.), intraportal (i.p.) and intragastric (i.g.) routes in rats in order to examine the potency of intestinal and hepatic extraction on the oral bioavailability of etoposide. And then investigated two flavonoids, quercetin and (-)-epigallocatechin gallate (EGCG), which are suggested to inhibit P-gp and CYP3A in vitro, on the bioavailability of etoposide in rats. The effects of these flavonoids on the pharmcokinetics of etoposide were compared with a well-known P-gp and CYP3A inhibitor, verapamil. A single dose of etoposide administered i.g. at a dose of 10 mg/kg, i.p. at a dose of 3.3 mg/kg or i.v. at a dose of 3.3 mg/kg to the male Sprague–Dawley rats, and a single verapamil at doses of 2 or 6 mg/kg, or quercetin at doses of 3, 12 and 20 mg/kg, or EGCG at doses of 3, 12 and 20 mg/kg was i.g. administered 30 min prior to the i.g. or i.v. administration of etoposide, respectively. Plasma concentration of etoposide was

determined by a HPLC equipped with a fluorescence detector.

After an i.v. administration of etoposide, the area under the plasma concentraion-time curve ($AUC_{0-\infty}$) of etoposide was 4830 ± 754 ng·h·ml^{1}, which was not significantly ($p > 0.05$) different from i.p. group (4769 ± 548 ng·h·ml^{-1}). The absolute bioavailability (F) of etoposide was 0.987 in i.p. dosing, which indicates that i.p. administered etoposide would not subject to the hepatic first-pass extraction considerably. After an i.g. administering etoposide at a dose of 10 mg/kg, the dose-normalized (based on a dose of 3.3 mg/kg of etoposide) $AUC_{0-\infty}$ value of etoposide was 404 ± 50.8 ng·h·ml^{1}, which was significantly lower ($p < 0.01$) than i.p. dosing. F value of etoposide was 0.084 in i.g. group, suggesting approximately 92% of etoposide failed to access the systemic circulation. In comparison of the hepatic first-pass effect, the intestinal first-pass effect must be the more important cause to the low F value of etopolside in rats.

After i.v. administration of etoposide in the presence of verapamil at doses of 2 and 6 mg/kg, the total body clearance (CL_t) of etoposide was significantly lower ($p < 0.01$, approximately 27.5%), and the $AUC_{0-\infty}$ of etoposide was significantly greater ($p < 0.01$, 37.7%–38.4%) than the i.v. control (given i.v. etoposide alone), which suggests the enhanced bioavailability of etoposide is mainly due to the decreased metabolism and excretion mediated mainly by CYP3A and P-gp in the liver and kidney. Preadministered verapamil altered the i.g. administered etoposide as well. In the presence of verapamil at doses of 2 and 6 mg/kg, the total body clearance (CL/F) of etoposide was significantly lower ($p < 0.01$, 27.8–31.2%), and the $AUC_{0-\infty}$ of etoposide was significantly greater ($p < 0.05$ at 2 mg/kg, $p < 0.01$ at 6 mg/kg, 39.2–47.6%) than the i.g. control (given i.g. etoposide alone). F value of etoposide elevated 1.39– to 1.48–fold in the presence of verapamil. Since etoposide subjects to extensive intestinal extraction, the enhanced oral bioavailability suggests the inhibited CYP3A and P-gp function in the intestine.

When pretreated with quercetin, the pharmacokinetic parameters of etoposide altered significantly in i.g. group but not in i.v. group, which could attribute to the quite low oral bioavailability of quercetin. In the presence of 3 and 12 mg/kg of quercetin, the CL/F of etoposide was significantly lower ($p < 0.01$, 27.6–33.7%) and the $AUC_{0-\infty}$ of etoposide was significantly greater ($p < 0.01$, 41.7–54.0%) than i.g. control group. Consequently, F value of etoposide elevated 1.42– to 1.54–fold, which was comparable with 2 and 6 mg/kg

of verapamil. Although orally administered quercetin subjects to extensive first-pass effect, it is absorbed almost completely in the intestine. The greater F value of etoposide should contribute to the property of quercetin of inhibiting P-gp and CYP3A in the intestine. Quercetin at a dose of 20 mg/kg decreased the CL/F and increased the $AUC_{0-\infty}$ of etoposide, but they were not significant.

When pretreated with another flavonoid, EGCG, the pharmacokinetic parameters of etoposide altered significantly both in i.v. and i.g. routes. In the presence of 12 mg/kg of EGCG, the CL_t of etoposide was significantly lower ($p < 0.05$, 25.1%), and the $AUC_{0-\infty}$ of etoposide was significantly greater ($p < 0.05$, 33.4%) than the i.v. control group, which is comparable with verapamil at doses of 2 and 6 mg/kg. 3 mg/kg of EGCG did not significantly alter the pharmacokinetic parameters of i.v. administered etoposide, which might be due to the low oral bioavailability of EGCG. When etoposide was administered intragastrically in the presence of EGCG, the CL/F of etoposide significantly lower (30.5–43.9%, $p < 0.01$), and the $AUC_{0-\infty}$ of etoposide was significantly greater (44.9–81.6%, $p < 0.01$ at 3 and 12 mg/kg, $p < 0.05$ at 20 mg/kg), and the peak plasma concentration (C_{max}) of etoposide was significantly higher (48.1–80.1%, $p < 0.01$ at 3 mg/kg, $p < 0.05$ at 12 and 20 mg/kg) than the i.g. etoposide alone. F values of etoposide in the presence of EGCG were 1.44– to 1.81–fold higher than the i.g. control group. The presence of EGCG reduced the CL/F and increased the $AUC_{0-\infty}$ of i.g. administered etoposide more than verapamil, specifically at a dose of 3 mg/kg.

The enhanced oral bioavailability of etoposide was observed in rats in combination of the natural flavonoids, quercetin and EGCG in this study. It was comparable with verapamil, a well–recommended P-gp and CYP3A inhibitor. It is possible that these natural flovonoids could act as candidates of modulators of P-gp and CYP3A to improve the oral bioavailability of etoposide in humans. The pharmacokinetic interaction between etoposide and quercetin or EGCG should be taken into consideration in the clinical setting to avoid the toxic reactions of etoposide.

Key words: Etoposide, verapamil, quecetin, (-)-epigallocatechin gallate (EGCG), P-glycoprotein (P-gp), CYP3A, pharmacokinetics, bioavailability, rats.

국 문 초 록

흰쥐에서 퀠세틴과 카테친이 에토포시드의 생체이용율에 미치는 영향

이 수 국
지 도 교 수: 최 준 식
조선대학교 대학원 약학과

생체내에서 수송체로 의한 약물 다제내성(Multidrug resistance, MDR)은 많은 항암약물의 항암작용에 주요 장벽이다. 경구투여 하였을 때 많은 항암약물들의 생체내이용률이 낮아서 사용이 불가능하다. 소장과 간에 존재하는 1 상 및 2 상반응의 대사효소(특히 CYP3A) 및 ATP-binding cassette (ABC) 수송체(특히 P-당단백질)등의 상가작용으로 인한 초회통과효과가 경구투여된 항암약물들의 낮은 생체내이용율의 주요원인이다. 에토포시드는 P-당단백질와 CYP3A 의 기질물질이다. 본 실험에서는 에토포시드를 경구, 문맥 및 정맥으로 투여시킨 다음 에토포시드의 약물동태학적 거동을 관찰하여 소장 및 간에서의 초회통과효과가 에토포시드의 약물동태에 미치는 영향을 관찰하였다. 시험관실험에서 프라보노이드류인 퀠세틴과 (-)-epigallocatechin gallate (EGCG)는 P-당단백질와 CYP3A 억제작용이 있다. 본 실험에서 흰쥐에게 에토포시드를 정맥 혹은 경구투여 30 분전에 퀠세틴 및 EGCG 를 경구투여시켰을 때 이들이 에토포시드의 약물동태에 미치는 영향을 연구하였으며, 그리고 이들의 영향력을 대표적인 P-gp 및 CYP3A 억제제인 베라파밀과 비교하였다. 웅성 Sprague-Dawley 흰쥐에게 에토포시드를 경구(10 mg/kg), 문맥(3.3 mg/kg) 및 정맥(3.3 mg/kg)으로 투여시켰다.

그리고 에토포시드를 경구(10 mg/kg) 혹은 정맥(3.3 mg/kg)투여 30 분전에 3, 12 및 20 mg/kg 퀠세틴, 3, 12 및 20 mg/kg EGCG, 2mg/kg 및 6 mg/kg 베라파밀을 각각 경구투여시킨 다음 혈장중 에토포시드의 농도를 형광검출기를 사용한 HPLC 에서 측정하였다.

정맥투여시켰을 때 에토포시드의 혈장농도곡선하면적($AUC_{0-\infty}$)은 4830 ± 754 $ng \cdot h \cdot ml^{-1}$ 이었으며, 문맥투여군에서는 4769 ± 548 $ng \cdot h \cdot ml^{-1}$ 으로서 정맥투여군에 비해 유의성($p>0.05$) 있게 변화되지않았다. 문맥투여군의 절대적 생체이용율(F)은 0.987 이며, 간에서 초회통과효과는 에토포시드의 생체내이용률에 큰 영향을 미치지 않았다. 경구투여하였을 때 에토포시드의 투여량을 3.3 mg/kg 을 기준으로 계산한 $AUC_{0-\infty}$값은 4042 ± 50.8 $ng \cdot h \cdot ml^{-1}$ 이었으며, 문맥투여군에 비해 유의성($p < 0.01$) 있게 감소되었다. 절대적생체이용율(F)은 0.084 이었으며, 약 92%의 에토포시드는 초회통과효과에 의해 소실되었다. 소장에서 초회통과효과가 간에 비해 에토포시드의 생체내이용률에 훨신 큰 영향을 주었다.

베라파밀을 전투여하였을 때 정맥 및 경구투여시킨 에토포시드의 약물동태학적 파라미터는 유의성 있게 변화되었다. 에토포시드를 정맥투여하였을 때 대조군(에토포시드 단독정맥투여)에 비해 전투여군에서 에토포시드의 전신클리어런스(CL_t)는 유의성 있게 감소되었고($p < 0.01$, 27.5%), $AUC_{0-\infty}$는 유의성 있게 증가되었다($p < 0.01$, 37.7–38.4%). 베라파밀은 간 및 신장에서 CYP3A 및 P-gp 을 억제시켜서 에토포시드의 생체내이용률을 증가시킨 것을 추측할 수 있다. 에토포시드를 경구투여 하였을 때 대조군(에토포시드 단독경구투여)에 비해 베라파밀 전투여군에서 전신클리어런스(CL/F)는 유의성 있게 감소되었으며($p < 0.01$, 27.8–31.2%), $AUC_{0-\infty}$는 유의성 있게 증가되었다(39.2–47.6%, 2 mg/kg 에서 $p < 0.05$, 6 mg/kg 에서 $p < 0.01$). F 갑은 단독투여군에 비해 1.39–1.48 배로 증가되었다. 증가된 에토포시드의 생체내이용율은 주로 베라파밀이 소장에서 CYP3A 과 P-gp 을 억제시켜 증가된 것을 추측할수 있다.

퀠세틴을 전투여하였을 때 정맥투여시킨 에토포시드의 약물동태학적

파라미터는 유의성 있게 변화되지 않았으나 경구투여군에서는 유의성 있게 변화되었다. 에토포시드를 경구투여 하였을 때 대조군(에토포시드 단독 경구투여)에 비해 퀠세틴 전투여군에서 에토포시드의 CL/F 는 유의성 있게 감소되었으며($p < 0.01$, 27.6–33.7%), $AUC_{0-\infty}$는 유의성 있게 증가되었다($p < 0.01$, 41.7–54.0%). F 값은 1.42–1.54 배로 높았졌다. 경구투여하였을 때 퀠세틴의 생체이용률은 극히 낮아서 에토포시드 정맥투여군에는 영향을 미치지 않은 것이다. 그러나 소장에서 퀠세틴은 쉽게 흡수되어 장관막에서 CYP3A 및 P-gp 에 인한 에토포시드의 초회통과효과를 억제할 수 있다. 3 및 10 mg/kg 퀠세틴은 2 및 6 ma/kg 베라파밀과 동등하게 효율적으로 경구투여시킨 에토포시드의 생체내이용률을 증가시켰다. 20 mg/kg 퀠세틴은 에토포시드의 CL/F 를 감소 시키고 $AUC_{0-\infty}$를 증가시켰으나 통계학적으로 유의성은 없었다.

프라보노이드류인 EGCG 을 전투여하였을 때 경구 및 정맥으로 투여시킨 에토포시드의 약력학적 파라미터는 유의성 있게 변화되었다. 정맥대조군에 비해 12 mg/kg EGCG 전투여군에서 에토포시드의 CL_t 는 유의성 있게 감소되었으며($p < 0.05$, 25.1%), $AUC_{0-\infty}$는 유의성 있게 증가되었다($p < 0.05$, 33.4%). 이 결과는 베라파밀이 에토포시드에 미치는 영향력과 유사하다. 3 mg/kg EGCG 는 에토포시드에 대하여 유의성 있는 변화를 초래하지 않았다. 에토포시드를 경구투여시켰을 때 대조군에 비해 전투여군에서 CL/F 는 유의성 있게 감소되었고($p < 0.01$, 30.5%–43.9%), $AUC_{0-\infty}$는 유의성 있게 증가하였으며(44.9–81.6%, 3 및 12 mg/kg 에서 $p < 0.01$, 20 mg/kg 에서 $p < 0.05$), 최고혈중농도(C_{max})도 유의성 있게 증가되었다(48.1–80.1%, 3 mg/kg 에서 $p < 0.01$, 12 mg/kg 및 20 mg/kg 에서 $p < 0.05$). F 갑은 1.44–1.81 배로 높아졌다. 베라파밀에 비해 EGCG(특히 3 mg/kg 에서)는 에토포시드의 약력학적 파라미터에 더욱 큰 영향을 미치었다.

본 연구에서 흰쥐에게 프라보노이드류인 퀠세틴 혹은 EGCG 를 함께투여시켰을 때 경구투여시킨 에토포시드의 생체내이용률이 현저히 높아졌다. 증가된 생체내이용률은 P-gp 및 CYP3A 억제제인 베라파밀의 효률과

유사하였다. 프라보노이드류들은 천연음식물에 흔이 존재하는 물질로서 인체에서 많은 유익한 작용이 있으며 지속적인 독성작용이 없다. 그리하여 경구용 에토포시드를 퀠세틴 혹은 EGCG 와 같은 화합물질들과 함께 조합하면 균일하지않은 에토포시드의 생체내이용율을 개선시키는데 도움이 될 수 있으리라 사료된다. 그리고 퀠세틴과 EGCG 를 혹은 이들이 많이 함유한 음식물들을 에토포시드와 함께 섭취할 때 에토포시드의 투여량을 조정하는 것이 바람직하다고 사료된다.

1. INTRODUCTION

The resistance of various human tumors to multiple chemotherapeutic drugs (multi-drug resistance, MDR) is a major barrier for the therapeutic effect of cancer therapy (Gottesman and Pastan, 1993). MDR is a term used to describe the phenomena that tumor cells resistant a number of structurally and functionally unrelated chemotherapeutic agents. The phenomena of MDR in mammalian cells have been broadly classified into two mechanisms; the cellular and non-cellular mechanisms (Fan et al., 1994). Non-cellular MDR are typically associated with solid tumors which exhibit unique physiological properties compared to circulating tumors, such as the blood vessels in the tumors are dilated, tortuous, and saccular, and the interstitial fluid pressure increased compared to the normal tissues due to higher vascular permeability and absence of a functional lymphatic system (Jain, 1987), which can result in a decrease in the accumulation of anticancer drugs in these regions. The hypoxic condition within tumors induces the increased lactic acid conferred resistance for weak bases, where cellular uptake is dependent on the pH gradient across membranes (Demant et al., 1990). Cellular MDR is classified into two major phenotypes: non-classical MDR phenotypes and transport-based classical MDR phenotypes. The term non-classical MDR is used to describe non-transport-dependent resistance, which caused by specific enzyme systems, such as glutathione *S*-transferase and topoisomerase, to decrease the cytotoxic activity of drugs independent of intracellular drug concentrations.

The transport-based classical MDR is caused by the ATP-binding cassette (ABC) family, a membrane transport ATPases. The general structures of ABC transporters compose of 12 transmembrane (TM) regions, split into two ‘halves’, each with a nucleotide-binding domain (NBD) (Fig. 1A), such as P-glycoprotein (P-gp, MDR1), MDR3, BSEP (SP-gp), multidrug resistance-associated protein (MRP) 4, MRP5, and MRP8. MRP1–3 and MRP6–7 have an additional five TM regions at the N-terminus (Fig. 1B). Breast cancer resistance protein (BCRP) has only six TM regions and one NBD (Fig. 1C), which was proposed to function as a dimer (Ozvegy et al., 2001). NDBs play a role in cleaving ATP (hydrolysis) to derive energy necessary for transporting cell nutrients, such as sugars,

amino acids, ions and small peptides across membranes.

P-gp, an important member of ABC family, is highly expressed in solid tumours of epithelial origin, such as the colon (Cordon-Cardo et al., 1990), kidney (Fojo et al., 1987a), and breast (Merkel et al., 1989) to efflux substrates out of cells. The tumor cells expressing P-gp reduced intracellular concentrations of the substrate drugs which decreased the cytotoxicity of a broad spectrum of antitumor drugs including anthracyclines (e.g. doxorubicin), vinca alkaloids (e.g. vincristine), podophyllotoxins (e.g. etoposide) and taxanes (e.g. paclitaxel). MRPs, another important member of the ABC family, has been described as a Vanadate-sensitive magnesium-dependent glutathione S-conjugate (GS-conjugate) ATPase (GS-X pump) capable of transporting organic anion drug conjugates as well as intact anticancer drugs (Grant et al., 1994; Borst et al., 1997). Several isoforms of MRPs have been identified and the mainly mentioned are MRP1 and MRP2 (cannalicular multispecific organic anion transporter, cMOAT), which have been identified as organic anion transporters (Borst et al., 1997).

Since MDR is one of the main obstacles to successful chemotherapy of cancer, a number of biochemical, pharmacological and clinical strategies have been devised to overcome the deffence in the effect of anticancer drugs. One of the possible strategies for reversal of transport-based classical MDR is inhibition of the activity of these proteins. Some therapeutic agents were supposed to be the first generation MDR modulators, such as calcium channel blockers (verapamil, felodipine, nicardipine, nifedipine and diltiazem), quinolines, hormones, cyclosporines (cyclosporin A), surfactants, and antibodies (Ford and Hait, 1990; Ford and Hait, 1993). They could reverse MDR at concentrations much higher than those required for their individual therapeutic activity, which resulted in unnecessary adverse effects and toxicities. The second generation modulators, analogs of the first generation, were more potent and considerably less toxic, such as the analogs of verapamil, dexverapamil (less cardiotoxic *R*-enantiomer of verapamil), the non-immunosuppressive analog of Cyclosporin A, PSC 833, and others. The third generation of MDR modulators was developed using structure–activity relationships and combinatorial chemistry approaches targeted against specific MDR mechanisms, such as specific P-gp blockers, the acridonecarboxamide GF 120918 (Hyafil et al., 1993). Although these agents appear to be well tolerated in combination with anticancer drugs, it

is need to be determined whether these compounds are suitable for clinical application in anticancer therapy.

P-gp is also present at the normal tissues such as kidney and adrenal gland (high level), liver, small intestine, colon and lung (medium level), and prostate, skin, spleen, heart, skeletal muscle, stomach and ovary (low level) (Fojo et al., 1987b; Gatmaitan and Arias, 1993). Same as P-gp, MRP1 is highly expressed in intestine, kidney and lung, and lower in liver (Cherrington et al., 2002; Flens et al., 1996; Zaman et al., 1993) and MRP2 is expressed mainly in liver, intestine, and kidney tubules (Fromm et al., 2000; Schaub et al., 1997). As shown in Figure 17, P-gp and MRPs spreaded in the excretory organs provide a barrier to eliminate the substrates out of the body. P-gp and MRP2 co-localized to the apical membrane of the intestine, liver, kidney, and blood–brain barrier (Thiebaut et al., 1987; Buchler et al., 1996; Fromm et al., 2000; Schaub et al., 1999), and MRP1 is localized to the basolateral membranes of polarized epithelial cells of the intestinal crypt (Peng et al., 1999), renal distal and collecting tubules (Peng et al., 1999), and liver (Mayer et al., 1995; Roelofsen et al., 1997).

P-gp and MRPs are reportedly co-localized with phase I and Phase II metabolizing enzymes, CYP3A4, UDP-glucuronosyltransferases, and glutathione-*S*-transferases in the liver, kidney and intestine (Sutherland et al., 1993; Turgeon et al., 2001) (Figure 17). The CYP3A subfamily involves in approximately 40–50% of phase I metabolism of marketing drugs (Guengerich, 1995). Specifically, CYP3A4 accounts for 30% of hepatic CYP and 70% of small intestinal CYP (Schuetz et al., 1996). A substantial overlap in substrate specificity exists between CYP3A4 and P-gp (Wacher et al., 1995). Additionally, the phase II conjugating enzymes, such as UDP-glucuronosyltransferases and glutathione-*S*-transferases, may subsequently modify either the phase I metabolites or the parent compounds as the conjugated compounds, and further subject toMRP2-mediated efflux in the liver and intestine. Thus, a synergistic relationship exists between the transporters and metabolic enzymes, such as CYP3A4 versus P-gp and conjugating enzymes versus MRP2, within excretory tissues to protect the body against invasion by foreign compounds, which also decrease the oral bioavailability of many drugs, especially anticancer drugs.

Oral administration of drugs has many advantages over intravenous injection because it is less invasive, easier to use for the patient in a chronic regimen and more cost-effective

because of decreased hospitalization. The small intestine represents the principal site of absorption for orally administered compounds. There are two principal pathways, paracellular and transcellular, in the intestinal epithelium that allows the compounds to cross. Some small hydrophilic, ionized drugs are absorbed via the paracellular pathway for there small particle size is suitable for pass through the tight intercellular junctions (Hayashi et al., 1997). Many orally administered drugs are lipophilic and undergo passive transcellular absorption (Hunter and Hirst, 1997). Drugs that cross the apical membrane or present in the blood would be substrates for apical efflux of transporters, specifically ABC proteins such as P-gp and MRP2, and cytochrome P450 (especially CYP3A4)-mediated Phase I metabolism of orally ingested compounds (Watkins, 1992). Phase I and phase II metabolic enzymes may yield metabolites that are themselves substrates for efflux pumps, such as P-gp and MRP2 (Keppler et al., 1999). The fraction of compounds that escapes this first barrier will pass to the liver via the portal vein and subject to further metabolism and biliary excretion by the same enzymes and transporters present in the enterocytes, which complete the first cycle of enterohepatic circulation (first-pass extraction). Drugs that reach the systemic circulation following first pass extraction by the liver, or through the lymphatics, will meet the kidneys, which are also well equipped with the efflux transporters for the active excretion of the parent or the metabolites of the compounds. The efflux transporters and intracellular metabolic enzymes in the intestine and liver are critical determinants of overall oral bioavailability.

Etoposide or VP-16-213 (4'-demethylepipodophyllotoxin-9-(4,6-O-ethylidene)-β-D-glucopyranoside) is a semisynthetic derivative of podophyllotoxin, a naturally occurring compound extracted from the roots and rhizomes of the plants *Podophyllum peltatum* or *Podophyllum emodi* (Stahelin et al., 1991; Clark and Slevin, 1987). Etoposide is used in the treatment for a wide range of malignancies (*e.g.*, small cell lung cancer, acute leukemia, lymphoma, testicular cancer) as a single agent or one of the constituents of standard therapeutic regimens (Clark and Slevin, 1987). It exerts its anticancer action via inhibition of topoisomerase II enzyme and/or induction of direct DNA breaks (Wozniak and Ross, 1983). Etoposide is a chiral drug and can be degraded from the *trans-isomeric* form of the lactone to the *cis*-lactone in neutral, weak acidic and alkaline conditions (Figure 2A and B). The stereochemistry of the *trans*-lactone is essential for therapeutic activity of

etoposide (Dow et al., 1983). Metabolism of etoposide includes cytochrome P450-catalyzed *O*-demethylation in rodents (Haim et al., 1987; van Maanen et al., 1987) and in humans (Relling et al., 1992; Relling et al., 1994) of the dimethoxyphenol pendant ring, which forms the etoposide catechol (Figure 2C). This process is mediated mainly by CYP3A4 and to a minor extent by CYP1A2 and 2E1 (Kawashiro et al., 1998). Etoposide is approximately equally excreted in urine and bile (Lum et al., 1992). Approximately 20–35% of the etoposide dose is excreted unchanged in the urine and ~2% in bile (Relling et al., 1994). Approximately 94% of etoposide is bound to plasma protein (Allen and Creaven, 1975). As other anticancer agents, the toxicity of etoposide includes hematological toxicity (myelosuppression), gastrointestinal effects (nausea and vomiting), cardiovascular effects, and hepatotoxicity (McEvoy, 2000). Etoposide exhibits erratic bioavailability with a range of 25–75%, with considerable intra- and interpatient variation (Clark and Slevin, 1987). Several approaches failed to reduce the variability of etoposide, such as altering gastric pH, gastric emptying time, and coadministration of bile salts (Joel et al., 1995).

Etoposide is reported to be a substrate for P-gp (Pastan and Gottesman, 1991). Infusion of Cyclosporine A, a first generation of P-gp inhibitor, in rats treated intravenously with a single dose of etoposide showed the decreased plasma clearance, increased plasma and tissue concentrations of etoposide (Carcel-Trullols et al., 2004); Pretreatment of PSC 833, the second generation of P-gp-mediated MDR modulator, 30 min before the etoposide resulted in the increased toxicity and the enhanced bioavailability of etoposide in rats (Keller et al., 1992). Quinidine, a dual inhibitor of CYP 3A and P-gp, has shown the enhanced uptake of etoposide from rat *in situ* perfused intestinal loops (Leu and Huang 1995). According to the experimental results of Allen et al. (2003), etoposide is a substrate for BCRP-mediated resistance in vitro, but it is not a major limiting factor in oral uptake of etoposide based on the fact that GF120918, a dual P-gp and BCRP inhibitor, increased the plasma levels of etoposide by 4– to 5–fold after oral administration of etoposide in wild mice but not in P-gp-deficient mice. MRP2 also seems to be the minor factor as BCRP since MRP2 cDNA-transfected cells display high-level resistance to vincristine but only low-level to etoposide (Koike et al., 1997; Kawabe et al., 1999). Since ABC transporters and the metabolic enzymes, especially P-gp and CYP3A, are the major factors

impeding etoposide pass through enterohepatic circulation, it is possible that the dual inhibitors of P-gp and CYP3A might enhance the oral exposure of etoposide. As upper mentioned, although some P-gp modulators such as verapamil, cyclosporine A and PSC 833 is proved to be the potent P-gp inhibitors *in vitro*, but their toxicities hinder their use in clinical application (Bradshaw and Arceci, 1998). Some flavonoids as natural products were shown to extert as modulators of the ABC transporters (Castro and Altenberg, 1997; Scambia et al., 1994) and phase I and phase II metabolizing enzymes (Tsyrlov et al., 1994; Walle et al., 1995). Since they have many health promoting benefits and have no consistent side effects except for catechin, which can occasionally cause fever, anemia from breakdown of erythrocyte and hives (Bar-Meir et al., 1985; Conn, 1983), and could subside when treatment was discontinued, it could be expected as one of the nature modulators to improve the bioavailabilities of the anticancer drugs.

Flavonoids are widely distributed in dietary supplements such as vegetables, fruit, tea and wine (Hertog et al., 1993b). Flavonoids have many beneficial effects including antioxidant, antibacterial, antiviral, antiinflammatory, antiallergic, and anticarcinogenic actions (Ross and Kasum, 2002; Hodek et al., 2002) though whether these effects can be attributed to the aglycone forms or their metabolites is not entirely clear. The total daily intake of flavonoids via the dietary supplements has been 23 mg/day in Dutch population (Hertog et al., 1993a), among which the most important flavonoid was the flavonol quercetin (mean intake 16 mg/day). Many flavonoids are ubiquitous in all parts of the plant. Flavonoids are polyphenolic compounds possessing 15 carbon atoms; two benzene rings joined by a linear three-carbon chain (Figure 3A). A CHROMANE ring bearing a second aromatic ring B in position 2, 3 or 4 (Figure 3B). The oxygen bridge involving the central carbon atom (C_2) of the three-carbon chain occurs in a rather limited number of cases, where the resulting heterocyclic is of the FURAN type. Various subgroups of flavonoids are classified according to the substitution patterns of ring C. Both the oxidation state of the heterocyclic ring and the position of ring B are important in the classification. The major subgroups of flavonids are as followes (Figure 4): Flavonols (quercetin, morin, kaempferol, myricetin, rutin, isorhamnetin), Flavones (apigenin, luteolin, primuletin), Flavanones (hesperetin, hesperidin, naringenin, naringin, eriodictyol), Flavanols, also called catechins ((+)-catechin, (+)-gallocatechin, (-)-epicatechin, (-)-

epigallocatechin, (-)-epicatechin 3-gallate, (-)-epigallocatechin 3-gallate, theaflavin, theaflavin 3-gallate, theaflavin 3'-gallate, theaflavin 3,3'-digallate, thearubigins), Anthocyanidins (cyanidin, delphinidin, malvidin, pelargonidin, peonidin, petunidin) and Isoflavonoids (genistein and daidzein). Most of these (flavanones, flavones, flavonols, and anthocyanins) bear ring B in position 2 of the heterocyclic ring. In isoflavonoids, ring B occupies position 3.

Although there is strong evidence to suggest beneficial effects of flavonoids in human health, the extent and mechanism by which flavonoids reach the systemic circulation from dietary sources are controversial. Plant flavonoids are predominantly found as β-glycosides with flavonols (including quercetin) existing as 3, 7, and 4' *O*-glycosides, whereas other flavonoids, such as flavones, flavonones, and isoflavones, are mainly glycosylated at position 7 (Price et al., 1997; Fossen et al., 1998). Dietary flavonoids are deglycosylated by cytosolic β-glucosidase (CBG) and lactase phlorizin hydrolase (LPH) in the small intestine (Day et al., 1998; Day et al., 2000), followed by conjugation primarily with glucuronic acid in the small intestine epithelial cells (Figure 5) (Gee et al., 2000; Crespy et al., 1999; Spencere al., 1999). Ingested flavonoids undergo extensive Phase I and Phase II metabolism and are present in the circulation as a complex mixture of free aglycone with glucuronidated, methylated, and sulphated forms. However, cleavage by glucuronidases at several sites in the body can restore the aglycone form (Figure 5) (Murota and Terao, 2003) of which shows enhanced ability to partition across membranes and access intracellular sites due to its greater lipophilicity (Spencer et al., 2001).

Several studies have shown that flavonoids can modulate the activities of both P-gp and MRP1 (Zhang and Morris, 2003a; Bobrowska-Hagerstrand et al., 2003) affecting drug accumulation, cell viability following cytotoxic drug exposure, and the ATPase activity of P-gp (Bobrowska-Hagerstrand et al., 2003). Some flavonoids have been reported to interact with the intrinsic ATPase of P-gp, both inhibition and stimulation of P-gp ATPase activity have been observed for silymarin, morin, and biochanin A (Zhang and Morris, 2003b). Since P-gp located in the apical membrane (Anderle et al., 1998) and some mRNAs of organic cation transporters (OCT) has also been detected (Martel et al., 2001), the monolayers formed by a human colon carcinoma cell line, Caco-2 cell, is used for the study of membrane permeability, specifically for the transport characterization of the

intestinal epithelium. Some flavonoids reduced the secretory flux of talinolol across Caco-2 cells, such as hesperetin, quercetin, kaempferol, spiraeoside, isoquercitrin and naringin, but none of the selected flavonoids was able to replace [^{3}H]talinolol from its binding to P-gp, which might be due to an interaction with P-gp without competition of talinolol binding site of P-gp (Ofer et al., 2005). Several flavonoids, specifically methoxylated flavonoids, are confirmed to be the good inhibitors of MRP1 and 2 (van Zanden et al., 2004).

The flavonol quercetin (3,5,7,3',4'-pentahydroxyflavanone) is one of the most prevalent flavonoids. It presents in fruits, vegetables and beverages mainly as glucosides, with the highest content in onions, apples and red wine (Kiviranta et al., 1988; Hertog et al., 1992; Hertog et al., 1993a). Epidemiological data have demonstrated that consumption of diet rich in quercetin would reduce the risk of mortality from coronary heart disease (Hertog et al., 1993b) and the risk of stroke (Keli et al., 1996). In addition, quercetin and quercetin monoglucosides have been shown to inhibit 15-lipoxygenase, an enzyme thought to play a role in the oxidative modification of low density lipoprotein, leading to foam cell formation in the early development of atherosclerosis (Luiz et al., 1998). The daily dietary intake of quercetin ranges from 4 to 68 mg based on epidemiological studies in the U.S., Europe, and Asia (Knekt et al., 1997, Hertog et al., 1995, Hertog et al., 1993a and Rimm et al., 1996). It can reach several hundred mg in dietary supplement and several grams in anticancer therapy (Lamson and Brignall, 2000). Chemical structures of quercetin aglycone, glucoside and its metibolites are shown in Figure 5.

The oral bioavailability of quercetin is quite low. When pigs received a single oral dose of 148 μmol/kg (equivalent to 50 mg/kg) of quercetin aglycone, quercetin-3-*O*-glucoside (Q3G) or quercetin-3-*O*-glucorhamnoside (rutin) as part of their diet, the main metabolite in plasma was always conjugated quercetin which were detected only after β-glucuronidase/sulfatase treatment of the samples, whereas free quercetin was not detected in either the jugular or the portal blood (Cermak et al., 2003). It was consistent with the report showed by Ader et al. (2000) that the absolute bioavailability of free unchanged quercetin was 0.54 ± 0.19%, and it was considerably increased to 8.6 ± 3.8% after taking into account of the conjugated quercetin and further increased to 17.0 ± 7.1% by including quercetin's metabolites (isorhamnetin, tamarixetin, kaempferol) when pigs were treated

with an oral dose of 50 mg/kg of quercetin. The all administered flavonols must have undergone nearly complete metabolism in the intestinal mucosa. In humans and rats, catechol-*o*-methyltransferase and UDP-glucuronosyltransferase which located in the mucosa of the small and large intestine were able to metabolize different flavonoids (Cheng et al., 1999; Piskula and Terao, 1998) (Figure 5), the intestine possesses the capability to methylate and glucuronidate flavonols. The plasma metabolite level reached its peak in < 1 h after the ingestion of onions or Q4G, whereas after the intake of rutin, metabolite plasma levels peaked only after 6–9 h (Hollman et al., 1997; Graefe et al., 2001; Hollman et al., 1999). This indicates that quercetin glucosides were absorbed from the upper small intestine, whereas rhamnoside was not absorbed until it reached the terminal ileum or even the large intestine. Like the monoglucosides, the quercetin aglycone itself was readily absorbed in the small intestine in rats (Manach et al., 1997).

Quercetin showed the potency to modulate CYP3A catalyzed metabolism and the ABC family, specifically P-gp, mediated transport *in vitro*. In human liver microsomal samples, Quercetin inhibited CYP3A4-mediated 3-hydroxylation of quinine, which was greater than naringenin and naringin at the same concentration of 100 μM, and flavonoids with more phenolic hydroxyl groups produced stronger inhibition than those with less hydroxyl groups (Ho et al., 2001). Quercetin and kaempferol caused substantial inhibition of CYP3A4-mediated metabolism of cortisol in Caco-2 cells (Patel et al., 2004) and exhibited a remarkable inhibition of P-gp-mediated efflux of ritonavir, a substrate for P-gp and/or CYP3A4, by increasing its cellular uptake in Caco-2 cells, which were comparable with the inhibitory effect of quinidine, a well-known inhibitor of P-gp (Patel et al., 2004). In an everted rat gut sac, quercetin inhibited the activity of intestinal P-gp (Hsiu et al., 2002). The *in vitro* outcome has been applied to the *in vivo* study. Digoxin is extensively metabolized in rats by CYP 3A (Salphati and Benet, 1999). In contrast to rats, digoxin is a substrate for P-gp but not for CYP 3A enzyme in humans (Harrison and Gibaldi, 1976). The coadministration of 40 mg/kg of quercetin with 0.02 mg/kg of digoxin in pigs significantly elevated the C_{max} of digoxin by 413% and increased the $AUC_{0\text{-}t}$ by 170% (Wang et al., 2004). Coadminstration of 10 mg/kg of quercetin with 0.2 mg/kg of moxidectin subcutaneously in lamps significantly increased the AUC of moxidectin, a P-gp and CYP3A substrate (Dupuy et al., 2003). Prolonged exposure (10-day treatment) of

quercetin showed the significant increase of mRNA expression of both P-gp and CYP3A4 levels in Caco-2 cells (Patel et al., 2004), which might adversely promote the efflux and metabolism of the substrates.

HepG2 cells are a well-characterized immortalizd liver cell line of human origin and provide a useful model system for investigating human hepatic drug metabolism (Knasmuller et al., 1998). MRP2 is highly expressed, with low-level of MRP1, in HepG2 cells (Jedlitschky et al., 1997; Walle et al., 1999a; Walle et al., 1999b; Lee et al., 2001). In the HepG2 hepatic cell model, quercetin-7- and quercetin-3-glucuronides (Figure 5), the major products of small intestine epithelial cell metabolism (Gee et al., 2000), is metabolized by methylation of the catechol functional group of both quercetin glucuronides and hydrolyzed the glucuronide by endogenous β-glucuronidase followed by sulfation to quercetin-3′-sulfate (O'Leary et al., 2003). Efflux of quercetin metabolites from HepG2 cells (methylated glucuronide and sulfate conjugates) was not altered by verapamil, a P-gp inhibitor, but was competitively inhibited by MK-571, a selective inhibitor of MRP2, indicating a role for MRP2 in the efflux of quercetin conjugates from HepG2 cells (O'Leary et al., 2003). The metabolite of quercetin might be substrate for MRPs, specifically MRP2-mediated efflux. Accumulation of the established BCRP substrates mitoxantrone and bodipy-FL-prazosin was significantly increased by quercetin and other flavonoids, silymarin, hesperetin, daidzein, and the stilbene resveratrol (each at 30 μM) in BCRP-overexpressing cell lines rather than the respective wild-type cell lines (Cooray et al., 2004), suggesting the reversed BCRP-mediated efflux by quercetin and others.

Another important flavonoids, flavanols, also called catechins, are the major flavonoid found in green tea. Several studies illustrated that tea consumption might provide protection against stroke, osteoporosis, liver disease, and bacterial and viral infections (Mukhtar and Ahmad, 2000). Six catechins present in green tea, the most abundant being (−)-epigallocatechin gallate (EGCG) followed by (−)-epicatechin gallate (ECG), (−)-epigallocatechin (EGC), (−)-epicatechin (EC), (−)-catechin gallate (GC) and (+)-catechin (C) (Chu and Juneja, 1997). The chemical structures of catechins are shown in Figure 6. EGCG has a wide range of biological and pharmacological activities, including antioxidant (Higdon and Frei, 2003), antimutagenic, and anticarcinogenic activities

(Kuroda and Hara, 1999). A prospective cohort study of a Japanese population revealed that the daily intake of EGCG in green tea in these subjects was calculated to be 540–720 mg (Muto et al., 2001), which is about 9-12 mg/kg body weight.

EGCG is largely conjugated in the plasma of mice and rats, whereas EGCG exists mostly in free form in human plasma (Chen et al., 1997; Lee et al., 2002). When EGCG at a dose of 10 mg/kg was administered intravenously in rats, the $t_{1/2}$ of 135 min, clearance of 72.5 ml $\cdot kg^{-1} \cdot min^{-1}$ and V_d of 22.5 dl/kg were observed, and EGCG is mainly excreted through bile (Chen et al., 1997). A single oral EGCG at a dose of 2 mg/kg in humans showed T_{max} of 1.3–1.6 h and $t_{1/2}$ of 2.0 h in the plasma (Lee et al., 2002), and the bioavailability of EGCG is low. Chen et al. (1997) reported that the bioavailability of EGCG in rats after i.g. administration at a dose of 75 mg/kg was 1.6%. Cai et al. (2002) reported that the bioavailability of intraportal administered EGCG was 87%. These results suggests that the limited bioavailability of EGCG is due largely to the factors within the gastrointestinal tract such as limited membrane permeability, transporter mediated intestinal secretion, or gut wall metabolism.

EGCG and its metabolites showed the property to inhibit or substrate for the catalytic enzyme and the ABC transporters. EGCG and ECG inhibited CYP3A4 with the IC_{50} values of 10 and 30 μM, respectively (Muto et al., 2001). In addition, EGCG is a substrate for UDP-glucuronosyltransferase, sulfotransferase, and catechol-*O*-methyltransferase, and there are significant species differences in the amount of EGCG conjugate found in the plasma (Lu et al., 2003a; Lu et al., 2003b). The phase II metabolism and the efflux of EGCG and its metabolites affect the bioavailability of EGCG. According to the report of Hong et al. (2003), the presence of the MRP inhibitors indomethacin increased EGCG, 4″-*O*-methyl EGCG, and 4′,4″-di-*O*-methyl EGCG levels by 13–, 11–, and 3–fold in MDCKII/MRP1 cells, respecitively, and accumulation of EGCG and its methyl metabolites was also increased nearly 10-fold in the presence of MRP inhibitor MK-571 in MDCKII/MRP2 cells. However, they were not affected by GF120918, a third generation P-gp inhibitor, in P-gp overexpressing MDCKII cells, indicating that EGCG and its methyl metabolites are substrates for MRP1 and MRP2, but not for P-gp. Based on the location of MRP2 (apical) and MRP1 (basolateral) in the intestine, kidney and liver, they would act adversely to the bioavailability of their substrates. It was reported that the transcript level

of MRP2 was over 10-fold higher than that of MRP1 in the human jejunum (Taipalensuu et al., 2001), MRP2 might also paticipate in lowering the bioavailability of EGCG in the intestine. Although EGCG is not the substrate of P-gp, the inhibitory effect of EGCG on P-gp was observed in human Caco-2 cells. 100 μM of EGCG and the 10 μM PSC 833 (P-gp inhibitor) increased the apical-to-basal flux of [^{3}H]vinblastine across the Caco-2 cell monolayer by 2.6–fold and increased the accumulation of [^{3}H]vinblastine within the cells by 2.2– and 3.4–fold (Jodoin et al., 2002), respectively. EGCG also increased the intracellular accumulation of doxorubicin in human oral epidermoid carcinoma KB-A_1 cells overexpressing P-gp, the expression of *MDR1* mRNA was not changed obviously by increasing EGCG concentrations (Qian et al., 2005). This result indicates that EGCG increases intracellular drug level by modulating P-gp function, not by down-regulating *MDR1* gene transcription and P-gp expression. The ability of EGCG to reverse MDR in vivo was also evaluated in KB-A_1 in combination with cytotoxic agent doxorubicin (Zhang et al., 2004). Neither doxorubicin alone nor EGCG alone had any significant effect on the mass of the resistant tumors. In contrast, the combination of doxorubicin with EGCG significantly reduced the tumor mass. These results indicate that EGCG is capable of reversing doxorubicin resistance in vitro, and had no independent cytotoxic effects on tumor cells.

The flavonoids, quercetin and EGCG, are abundant in our dietary supplements. There are many opportunities that these flavonoids would be administered concomitantly with the agents that are substrates for CYP3A and P-gp in the clinical practice. Since they possess the ability to inhibit CYP3A and P-gp, they might affect the pharmacokinetics of many substrate agents. In this study, the pharmacokinetic behavior of etoposide after intragastric, intraportal and intravenous administration to rats was investigated to determine the extent of presystemic intestinal and hepatic extraction on the oral bioavailability of etoposide, and examined the effect of quercetin and EGCG on the oral bioavailability of etoposide in rats. Verapamil as a dual inhibitor of CYP3A and P-gp should affect the pharmacokinetics of etoposide in vivo. The potency of two flavonoids on the systemic exposure of etoposide was compared with that of verapamil.

2. MATERIALS AND METHODS

2.1. Materials

Etoposide, podophyllotoxin, quercetin dihydrate, (-)-epigallocatechin gallate (EGCG) and (±)-verapamil were purchased from Sigma Chemical-Aldrich Corporation (St. Louis, MO, USA). Injectable etoposide (20 mg/ml) was purchased from the Boryung Chemical Company (Seoul, Korea). HPLC grade methanol and tert-butylmethylether were acquired from Merck Company (Darmstadt, Germany). All other chemicals for this study were of reagent grade and were used without further purification. Water was deionized and filtered through a Millipore Milli-Q system (Bedford, MA, USA).

2.2. HPLC analysis

2.2.1. Instrumentation

A high performance liquid chromatograph equipped with a Waters 1515 isocratic HPLC pump, a Waters 717 plus autosampler and a Waters™ 474 scanning fluorescence detector (Waters Company, Milford, MA, USA). Data were acquired and processed with breeze™ Software (Version 3.2) (Waters Company).

2.2.2. Chromatographic conditions

Chromatographic separations were achieved using a Symmetry® C_{18} column (4.6 mm i.d. × 150 mm long; particle size 5 μm, Waters Company), and a μBondapak™ C_{18} HPLC precolumn (particle size 10 μm; Waters Company) was connected before the analytical column. The mobile phase consisting methanol-deionized water-acetic acid (50:50:0.5, v/v/v) was passed through a 0.45-μm membrane filter and degassed by a Bransonic® Ultrasonic Cleaner (Branson Ultrasonic Company, Danbury, CT, USA) under vaccum before use. The flow-rate of the mobile phase was maintained at 1.0 ml/min. Chromatography was performed at a temperature of 30˚C using a HPLC column temperature controller (Phenomenex Inc., CA, USA). The fluorescence detector was

operated at an excitation wavelength of 230 nm with an emission cut-off filter of 330 nm.

2.2.3. Preparation of stock solutions

Stock solutions of etoposide and podophyllotoxin (an internal standard) were prepared by dissolving 10 mg of each drug in 10 ml of methanol. All solutions were stored in a –40°C freezer (MDF-292, Sumwon Company, Seoul, Korea).

2.2.4. Preparation of analytical standard solutions

Standard solutions were prepared by diluting the stock solution with methanol immediately prior to use. All preparations were made in 1.5-ml polyethylene mocrotubes (Axygen Scientific Company, Calif., USA). Stock solution was diluted with methanol to obtain the concentrations required for preparation of standard solutions. The standard solutions of etoposide were 40, 80, 200, 400, 800, 2,000, 4,000 and 8,000 ng/ml. For podophyllotoxin, its standard solution was 50 ng/ml.

2.2.5. Sample preparation

The plasma concentrations of etoposide were determined by a HPLC assay method reported by Liliemark et al. (1995) and Manouilov et al. (1998) after a slight modification. Briefly, a 0.5-μl aliquot of 50-ng/ml podophyllotoxin and a 1.2-ml aliquot of tert-butylmethylether were mixed with a 0.2-ml aliquot of the plasma sample in a 2.0-ml polypropylene microtube (Axygen Scientific Company, Calif., USA). The resulting mixture was mixed vigorously with a vortex-mixer (Scientific Industries Company, NY, USA) for 1 min and centrifuged at 13,000 rpm for 10 min in a high-speed micro centrifuge (Hitachi Company, Tokyo, Japan). A 1.1-ml aliquot of the upper layer was transferred to another clean microtube, evaporated under nitrogen gas at 38˚C in a MG 2100 Eyela dry thermo bath (Rikakikai Company, Tokyo, Japan). A 0.2-ml aliquot of 50% methanol in deionized water was used to reconstitute the residue, and a 50-μl aliquot was injected directly onto the HPLC system.

2.2.6. Validation procedures

2.2.6.1. Linearity

Standard calibration curves were constructed by adding a 50-µl aliquot of etoposide standard solutions at the concentrations of 40, 80, 200, 400, 800, 2,000, 4,000 and 8,000 ng/ml and a 50-µl aliquot of podophyllotoxin at a concentration of 50 ng/ml into a 0.2-ml aliquot drug-free rat plasma, respectively. Thus, the corresponding plasma calibration standards were 10, 20, 50, 100, 200, 500, 1000 and 2000 ng/ml of etoposide in plasma, respectively. These plasma samples were extracted as described above. Calibration curves of etoposide were constructed using the ratio of the peak area of etoposide and that of podophyllotoxin as a function of etoposide concentration in plasma. The linearity of the assay procedure was determined by calculation of a regression line using the method of least squares analysis.

2.2.6.2. Recovery

To determine the extraction efficiency, a 50-µl aliquot of the standard solutions of etoposide at the concentrations of 200, 800 and 4000 ng/ml were added separately to a 0.2-ml aliquot of blank plasma samples to yield concentrations of 50, 200 and 1000 ng/ml of etoposide in plasma. A 50-µl aliquot of podophyllotoxin at a concentration of 50 ng/ml also added to blank samples to make a concentration of 2.5 ng/ml in plasma. Each of these spiked blank plasma samples were treated as those in the sample preparation. The absolute recovery was calculated by comparing the peak areas of spiked plasma extracts with those of unextracted neat standards containing the same amount of etoposide or podophyllotoxin prepared in 50% of methanol in deionized water. Each measurement was made five times.

2.2.6.3. Intra- and inter-day variability and determination of LOD and LLOQ

Intra-day variability was obtained on five different rat's plasma samples using the same calibration curve in a day. Inter-day variability was obtained on five different days. The mean relative standard deviation (RSD) of the mean predicted concentration for the independently assayed standards provided the measure of precision. Accuracy was calculated by the percentage deviation of the mean predicted concentration of etoposide from the expected target value.

The limit of detection (LOD) was determined by greater than 3.0 for signal to noise

(S/N) ratios. The lower limit of quantification (LLOQ) was determined by spiking a 0.2-ml aliquot of blank rat's plasma with etoposide at the concentration of the lowest calibrator with a precision of 20% and accuracy of ± 20%. The LOD and LLOQ were measured on five different days.

The predetermined criteria for acceptance of both intra- and inter-day results were that the standard concentrations of etoposide had to be accurate within ± 15% of their nominal values as determined by the best-fit regression line except for the LLOQ, where ± 20% was acceptable. The correlation coefficient (r^2) also had to be 0.95 or better.

2.3. Animal experiments

Male Sprague−Dawley rats (weighing 270–300 g) of 7−8 weeks of age were purchased from Dae Han Laboratory Animal Research Company (Choongbuk, Korea), and were given free access to a commercial rat chow diet (No. 322-7-1) purchased from Superfeed Company (Gangwon, Korea) and tap water. The animals were housed, two per cage, at a temperature of 22 ± 2°C, and a relative humidity of 50–60%, under a 12:12 h light-dark cycle. The experiments were started after acclimation under these conditions for at least 1 week. The Animal Care Committee of Chosun University (Gwangju, Korea) approved the protocol of this study.

The rats were fasted for at least 24 h prior to the start of the experiments and had free access to tap water. Each animal was anaesthetized lightly with ether and the left femoral artery was cannulated using a polyethylene tube (SP45, 0.58 mm i.d., 0.96 mm o.d.; Natsume Seisakusho Company LTD., Tokyo, Japan) for blood sampling. The left femoral vein was also similarly canulated for i.v. injection, and the pyrolic vein was canulated using a polyethylene tube (SP 10, 0.28 mm i.d., 0.61 mm o.d.) for intraportal infusion.

2.4. Drug administration and sampe collection

2.4.1. Intravenous (i.v.) administration of etoposide

Etoposide (injectable form was diluted in 0.9% NaCl-injectable solution) at a dose of 3.3 mg/kg was injected (total injection volume of 1.5 ml/kg) over 1 min via the femoral

vein for i.v. control group (n = 6). Blood samples (0.45 ml) were collected into heparinized tubes via the femoral artery at 0 (to serve as a control), 0.017 (at the end of the infusion), 0.1, 0.25, 0.5, 0.75, 1, 2, 4, 6 and 8 h after the injection. The blood samples were centrifuged at 13,000 rpm for 5 min, and the plasma samples were stored at -40˚C until HPLC analysis. A 0.4-ml aliquot of 0.9% NaCl-injectable solution was injected through the cannula immediately after each blood sampling to replace blood loss followed with a 0.2-ml aliquot of heparinized 0.9% NaCl-injectable solution (20 units/ml) to flush the cannula to prevent blood clotting.

2.4.2. Intraportal (i.p.) administration of etoposide

Etoposide (the same solution that was used in the intravenous study) at a dose of 3.3 mg/kg was infused (total injection volume of 4.5 ml/kg) over 20 min via the pyrolic vein using Sage^{TM} Syringe Pump Model M361 (Orion Reasearch Inc., MA, USA) to rats (n = 6). Blood samples (0.45 ml) were collected into heparinized tubes from the femoral artery at 0 (to serve as a control), 0.1, 0.25, 0.5, 0.75, 1, 2, 4, 6, 8 and 10 h after the beginning of infusion. Other procedures were similar to those in the i.v. groups.

2.4.3. Intragastric (i.g.) administration of etoposide

Etoposide (the same solution that was used in the intravenous study) at a dose of 10 mg/kg was administered using injector equipped with a long blunt needle (feeding tube) to rats (total volume of 3.0 ml/kg, n = 6). Blood samples (0.45 ml) were collected into heparinized tubes from the femoral artery at 0 (to serve as a control), 0.1, 0.25, 0.5, 0.75, 1, 2, 4, 6, 8 and 10 h after the administration. Other procedures were similar to those in the i.v. route.

2.4.4. Preadministration of verapamil

Verapamil solutions at doses of 2 and 6 mg/kg were prepared by dissolving verapamil in distilled water (3.0 ml/kg), respectively. They were i.g administered using feeding tube 30 min prior to i.g. administration of etoposide at a dose of 10 mg/kg or i.v. administration at a dose of 3.3 mg/kg to rats (n = 6, each).

2.4.5. Preadministration of quercetin

Quercetin suspentions at doses of 3, 12 and 20 mg/kg were prepared by mixing quercetin in distilled water (3.0 ml/kg). They were i.g. administered through long blunt needle 30 min prior to i.g. at a dose of 10 mg/kg or i.v. at a dose of 3.3 mg/kg of etoposide to rats (n = 6, each).

2.4.6. Preadministration of EGCG

EGCG solution at doses of 3, 12 and 20 mg/kg were prepared by dissoving EGCG in distilled water (3.0 ml/kg). EGCG at doses of 3 and 12 mg/kg were pretreated 30 min prior to i.v. administration of etoposide at a dose of 3.3 mg/kg or pretreated at doses of 3, 12 and 20 mg/kg 30 min prior to i.g. administration of etoposide at a dose of 10 mg/kg (n =6, each).

2.5. Pharmacokinetic analysis

The following pharmacokinetic parameters were calculated using the noncompartmental method (WinNonlin software version 4.1, Pharsight Corporation, Mountain View, CA, USA). The area under the plasma concentration-time curve from time zero to the time of last measured (AUC_{0-t}) was calculated using the linear trapezoidal rule. The AUC zero to time infinity ($AUC_{0-\infty}$) was obtained by the addition of AUC_{0-t} and the extrapolated area determined by C_{last}/K_{el}, where C_{last} is the plasma concentration measured at the last time point. The terminal elimination rate constant (K_{el}) was calculated using the log-linear regression of the terminal phase of the plasma concentration-time curve, and the terminal half-life ($t_{1/2}$) was calculated by $0.693/K_{el}$. The peak plasma concentration (C_{max}) and the time to C_{max} (t_{max}) of etoposide in plasma were obtained directly from the experimental data. The total body clearance for i.v. route (CL_t) and for i.g. route (CL/F) was calculated from D/ $AUC_{0-\infty}$, where D is the dose of etoposide,. The mean residence time (MRT) was calculated by dividing the first moment of AUC ($AUMC_{0-\infty}$) by $AUC_{0-\infty}$. The apparent volume of distribution at steady state (V_{dss}) was estimated by the product of $MRT_{i.v.}$ and CL_t after i.v. dosing. The extent of absolute bioavailability (F) of the extravascular doses was determined by dividing the dose-normalized $AUC_{0-\infty}$ of the extravascular routes to

that of i.v. route.

2.6. Statistical analysis

Statistical analysis was conducted using a one-way ANOVA followed by *a posteriori* testing with the use of the Dunnett correction for comparing groups more than two, or using a Student's *t*-test for comparing between the two groups. Differences were considered to be significant at a level of $p < 0.05$. All data were expressed in terms of mean ± S.D.

3. RESULTS

3.1. Chromatographic separation

Figure 7 illustrates chromatograms of blank rat plasma samples (A), plasma samples collected after oral administration of verapamil (B) and etoposide (C) to rats. The retention times of podophyllotoxin (internal standard, IS) and etoposide were 4.5 and 11.1 min, respectively. The overall run time lasted 12 min. Quercetin, EGCG and verapamil did not interfer the detection of etoposide and podophyllotoxin in this method.

3.2. Validation characteristics of analysis

Figure 8 shows the calibration curve of etoposide constructed by plotting the ratio of the peak area of etoposide to that of podophyllotoxin as a function of the plasma etoposide concentrations (10, 20, 50, 100, 200, 500, 1000 and 2000 ng/ml). There is an excellent linearity over the range of 10–2000 ng/ml with a mean correlation coefficient of 0.999 (Figure 8). The typical equation describing the calibration curve in rat's plasma was $y = 0.00215\,x - 0.00383$, where y is the peak area ratio of etoposide to podophyllotoxine and x is the concentration of etoposide.

The recovery of etoposide after liquid-liquid extraction procedure was evaluated at three concentrations of 50, 200 and 1000 ng/ml. The average efficiency of extraction from rat plasma was 82.0%. The recovery of the internal standard, podophyllotoxin, was 82.2% when spiked concentration in rat plasma was 2.5 ng/ml (Table 1).

The LOD for etoposide in rat plasma defined as a signal-to-noise ratio of greater than three was 10 ng/ml. The LLOQ for etoposide in 0.2 ml rat's plasma was 10 ng/ml with an acceptable precision and accuracy (RSD: 11.5%, deviation: −4%, n = 5).

The intra- and inter-day assay accuracy and precision values are given in Table 2. The intra-day accuracy (deviation) was within 11.5% for all concentrations, and the intra-day precision (RSD) varied between 1.6 and 10.5%. The inter-day accuracy and precision were within 13.4 and 11.5%, respectively.

3.3. Pharmacokinetics of etoposide in rats after i.v., i.p. and i.g. administration

After i.v. (3.3 mg/kg), i.p. (3.3 mg/kg) and i.g. (10 mg/kg) administration to rats, the mean arterial plasma concentration–time profiles of etoposide are shown in Figure 9 and Table 3, the dose-normalized (based on the dose of 3.3 mg/kg) $AUC_{0-\infty}$ values of etoposide are shown in Figure 10.

After i.v. administration, the area under the plasma concentraion–time curve ($AUC_{0-\infty}$) of etoposide was 4830 ± 754 $ng \cdot h \cdot ml^{-1}$, which was not significantly different ($p < 0.05$) from i.p. administration (4769±548 $ng \cdot h \cdot ml^{-1}$). The extent of absolute bioavailability (F) of etoposide after i.p. administration was 0.987, indicating that hepatic first-pass effect of etoposide was not considerable.

The dose-normalized (based on a dose of 3.3 mg/kg) $AUC_{0-\infty}$ value of etoposide after i.g. administration was 404 ± 50.8 $ng \cdot h \cdot ml^{-1}$, which was significantly smaller ($p < 0.01$) than that of i.p. group. The F value of etoposide after i.g. administion was 0.084, suggesting 92% of i.g. administered etoposide failed to reach the systemic circulation. The intestinal first-pass effect of etoposide should be the main factors to low F of etoposide.

3.4. Effect of verapamil on the pharmacokinetics of etoposide

After i.v. administraion of etoposide at a dose of 3.3 mg/kg in the presence or absence of verapamil at doses of 2 and 6 mg/kg, the mean arterial plasma concentration–time profiles of etoposide are shown in Figure 10, and listed in Table 4, and some relevant pharmacokinetic paremeters are listed in Table 10. The presence of verapamil significantly altered the pharmacokinetic parameters of etoposide compared to the control group (given etoposide alone). In the presence of verapamil, the total body clearance (CL_t) of etoposide was significantly slower ($p<0.01$, approximately 27.5%), and the $AUC_{0-\infty}$ of etoposide was significantly greater ($p <0.01$, 37.7–38.4%). The greater systemic exposure of etoposide suggests the decreased metabolism and excretion in the liver and kidney by verapamil. There were no significant differences in the K_{el} and $t_{1/2}$ of etoposide in the presence of verapamil.

After administration with verapamil at doses of 2 and 6 mg/kg, the mean arterial plasma concentraiton–time profiles of i.g. administered etoposide are shown in Figure 11 and

lister in Table 5, and some pharmacokinetic paremeters are listed in Table 11. In the presence of verapamil, the total body clearance (CL/F) of etoposide was significantly slower ($p < 0.01$, 27.8–31.2%), and the $AUC_{0-\infty}$ (39.2–47.6%) of etoposide was significantly greater ($p < 0.05$ at 2 mg/kg, $p < 0.01$ at 6 mg/kg). Peak plasma concentration (C_{max}) of etoposide was significantly higher (45%, $p < 0.01$) in the presence of verapamil at a dose of 6 mg/kg. F value of etoposide elevated 1.39– to 1.48–fold in the presence of 2 and 6 mg/kg of verapamil. There were no significant differences in the time to C_{max} (T_{max}), K_{el} and $t_{1/2}$ of etoposide in the presence of verapamil. The enhanced oral bioavailaiblity of etoposide suggests that CYP3A-catalyzed metabolism and P-gp-mediated efflux of etoposide in the intestine is inhibited by verapamil.

3.5. Effect of quercetin on the pharmacokinetics of etoposide

After i.v. administration of etoposide at a dose of 3.3 mg/kg in the presence or absence of quercetin at doses of 3, 12 and 20 mg/kg, the mean arterial plasma concentration–time profiles of etoposide are shown in Figure 12 and listed in Table 6, pharmacokinetic parameters of etoposide are listed in Table 12. Although the presence of quercetin caused the slower CL_t and the greater AUC of etoposide, they were not significantly different. Other parameters such as the K_{el} and $t_{1/2}$ were also not altered significantly. This could be due to the fact that the oral bioavailability of quercetin is quite low, therefore the concentration of quercetin in the systemic circulation might be too low to affect the pharmacokinetics of i.v. administered etoposide.

After i.g. administration of etoposide at a dose of 10 mg/kg in the presence or absence of quercetin at doses of 3, 12 and 20 mg/kg, the mean arterial plasma concentration–time profiles of etoposide are shown in Figure 13 and and listed in Table 7, and some pharmacokinetic paremeters of etoposide are listed in Table 13. The presence of quercetin at doses of 3 and 12 mg/kg caused significantly ($p < 0.01$) slower CL/F (27.6–33.7%) and significantly ($p < 0.01$) greater $AUC_{0-\infty}$ (41.7–54.0%) of etoposide. Consequently, F values of etoposide elevated 1.42– to 1.54–fold, which was comparable to that of 2 and 6 mg/kg of verapamil (1.38– to 1.47–fold). The C_{max} of etoposide in the presence of 12 mg/kg of quercetin was significantly higher (39%, $p < 0.05$) than the i.g. control. The other

parameters, such as T_{max}, K_{el} and $t_{1/2}$ of etoposide in the presence of quercetin were not significantly different from control group. Although orally administered quercetin subjects to extensive first-pass effect, it is absorbed almost completely in the intestine. The enhanced oral exposure of etoposide could be attribute to the property of quercetin that it inhibits P-gp and CYP3A in the intestine. Although 20mg/kg of quercetin caused the slower CL/F and the greater $AUC_{0-\infty}$ of etoposide, they were not significant.

3.6. Effect of EGCG on the pharmacokinetics of etoposide

Afer i.v. administration of etoposide in the presence or absence EGCG at doses of 3, 12 and 20 mg/kg, the mean arterial plasma concentration–time profiles of etoposide are shown in Figure 14 and listed in Table 8, and some pharmacokinetic paremeters are listed in Table 14. The presence of EGCG at a dose of 12 mg/kg caused significantly ($p < 0.05$) slower CL_t (25.1%) and greater AUC (33.4%) of etoposide. The above results are comparable with verapamil at doses of 2 and 6 mg/kg (Table 10). There were no significant alterations of the K_{el} and $t_{1/2}$ of etoposide in the presence of EGCG. EGCG at a dose of 3 mg/kg has not shown significant alteration of the pharmacokinetic parameters of etoposide, which might be due to the low oral bioavailability of EGCG.

After i.g. administration of etoposide at a dose of 10 mg/kg in the presence or absence of EGCG at doses of 3, 12 and 20 mg/kg, the mean plasma concentration–time profile of etoposide are shown in Figure 15, and listed in Table 9, and some relevent pharmacokinetic parameters are shown in Table 15. The presence of EGCG caused significantly slower CL/F (30.5–43.9%, $p < 0.01$), and greater $AUC_{0-\infty}$ (44.9–81.6%, $p < 0.01$ at 3 and 12 mg/kg, $p < 0.05$ at 20 mg/kg) and higher C_{max} (48.1–80.1%, $p < 0.01$ at 3 mg/kg, $p < 0.05$ at 12 and 20 mg/kg) of etoposide. F value of etoposide in the presence of EGCG was elevated 1.44– to 1.81–fold. The presence of EGCG caused slower CL/F and greater $AUC_{0-\infty}$ of etoposide than verapamil, specifically at a dose of 3 mg/kg. There were no significant alterations in the T_{max}, K_{el} and $t_{1/2}$ of etoposide.

4. DISCUSSION

The plasma concentrations of etoposide were measured by a slight modification of the reported HPLC methods by Liliemark et al. (1995) and Manouilov et al. (1998). Podophyllotoxin instead of teniposide was used as an internal standard. Although phenyl column showed a good separation of etoposide and podophyllotoxin from endogenous substances at the temperature of 30°C, the retention times of etoposide and the internal standard were shortened gradually within one month even if the column is set at the room temperature of 22°C or lower. Since C_{18} column has been used in detection of etoposide by others (Manouilov et al., 1998; Shirazi et al., 2001), Phenyl column was substituted by Symmetry C_{18} column, which was much more stable and durable. In comparison of the extraction efficiency, tert-butylmethylether showed the better benifits than chlorform (Liliemark et al., 1995), actonitrile (Reif et al., 2001), dietyl ether (Shirazi et al., 2001) and ethyl acetate (Xie et al., 1998). At the emission wavelength of 330 nm, using the excitation wavelength of 230 nm increased the peak area of either etoposide or podophyllotoxin more, nearly 1.6-fold, than using that of 220 nm, and there is no corresponding increase of the peak area of endogenous substances. The wavelength of fluorescence detector has ever been adapted using the excitation of 290 nm and the emission of 320 nm in the paper of Kiya et al. (1992) in detection of etoposide. When it was applied to this study, the areas of etoposide and podophyllotoxin could be amplified to 0.43– and 0.93–fold, respectively, but the areas of the endogenous substances were enlarged and interferred the detection of etoposide more than using the excitation wavelength of 230 nm and the emission wavelength of 330 nm.

Using the modified HPLC method, the excellent separation of etoposide and the internal standard was demonstrated in the chromatograms (Figure 7). The method was linear over the concentration range of 10–2000 ng/ml with r^2 = 0.999 (Figure 10). The method was accurate and reproducible with accuracy and precision less than 13.4 and 11.5%.

The applicability of the validated method was examined in the pharmacokinetic study of etoposide following i.g. administration at a dose of 10 mg/kg, and i.p. and i.v. administratin at a dose of 3.3 mg/kg to male Sprague–Dawley rats. The assay was sensitive enough to measure the plasma drug level in these three routes of administration

to determine the bioavailability of etoposide since the last measured time in plasma were 8,10, and 10 h for i.v., i.g., and i.p. administration, respectively. The times are over 3–times of the terminal half-life of etoposide (the $t_{1/2}$ of 1.83 h for i.v., 3.11 h for i.p. and 2.75 h for i.g. administered etoposide).

Orally administered etoposide shows variable bioavailability, with the ranges of 25–75%, and considerable intra- and inter-patient variation (Clark and Slevin, 1987). Different approaches, such as altering gastric pH, gastric emptying time, and coadministration of bile salts, to reduce variability of bioavailability of etoposide have failed (Joel et al., 1995). Several presystemic processes could contribute to the low oral bioavailability of drugs or chemicals. These include low solubility in the gastrointestinal fluid, poor membrane permeability, degradation/metabolism in the gastrointestinal tract, transporter-mediated intestinal secretion/efflux process and presystemic intestinal and hepatic metabolism and elimination. Orally administered etoposide subjects to *O*-demethylation in rodents and in humans, which is mediated mainly by CYP3A4 (CYP3A1/2 in rats) and to a minor extent by CYP1A2 and 2E1 (Kawashiro et al., 1998). Etoposide is a substrate for the efflux of ABC tranporters as well, mainly for P-gp (Pastan and Gottesman, 1991), and in a lower extent resistance mediated by BCRP and MRP2 in vitro (Allen et al. 2003; Koike et al., 1997; Kawabe et al., 1999). P-gp-mediated efflux and and CYP3A-catalyzed-metabolism in the intestine and liver might be the critical determinants of oral bioavailability of etoposide.

Drugs administered directly into the hepatic portal vein needs to first pass through the liver before reaching the systemic circulation, whereas it is immediately present in the systemic circulation following the administration into a peripheral vein. The $AUC_{0-\infty}$ of etoposide following i.p. administration was calculated and compared with that of i.v. injection to determine the extent of hepatic first-pass extraction of etoposide. As shown in Figure 10, the $AUC_{0-\infty}$ of etoposide following i.v. administration was not significantly ($p > 0.05$) different from that of i.p. administration, which indicates that hepatic first-pass extration is not the major cause to the low F of etoposide. On the other hand, the dose-normalized $AUC_{0-\infty}$ value of etoposide following i.g. administration was significantly ($p < 0.01$) lower than i.p. group. Approximately 92% of orally administered etoposide failed to access the systemic circulation. Although CYP3A in the microsome of hepatocytes is 2- to

5-fold higher than the enterocyte (De Waziers et a1., 1990), and it can be greater when compares the total mass of microsomal protein in the intestinal mucosa with that in the liver. The lower level extraction of etoposide in the liver than in the intestine may appear incongruent with the relative abundance of CYP3A in the two organs. Following facts can be a clue to explain this discrepancy. First, most orally administered drugs must pass through the small intestinal membrane to access the systemic circulation, but it is not the case in the liver to access hepatocytes (Figure 17). Like other lipophilic drugs, most of etoposide is absorbed via the apical enterocytes of the villi of small intestine where full of CYP3A and P-gp rather than via the deep crypts with low level of CYP3A and P-gp or the splanchnic capillaries by paracellular transport, which attribute to the considerable exposure of etoposide in CYP3A and P-gp of the enterocyte (Figure 17). Second, although the protein binding is not correlated with the exposure in the enterocytes, it is of magnitude for the exposure in the hepatocytes because only free form can pass through the sinusoidal membrane of hepatocytes. The high level protein binding of etoposide (94%) should be one of the contributors to its low hepatic first-pass effect (Allen and Creaven, 1975). Last, the blood flow in the liver is 55.2 $ml \cdot min^{-1} \cdot kg^{-1}$ in rats, and in the gut is 30 $ml \cdot min^{-1} \cdot kg^{-1}$ (Davies and Morris, 1993). So, the blood flow in the small intestine must be considerably lower than that in the liver. The lower limit of blood flow would increase residence time of etoposide in the intestine during first-pass compared to hepatocyte, which can be another contributor to the high intestinal first-pass extraction of etoposide than the liver. Leu and Huang (1995) reported that quinidine, a dual inhibitor of CYP3A and P-gp, enhanced uptake of etoposide from rat *in situ* perfused intestinal loops. The factors within the gastrointestinal tract such as transporter mediated intestinal secretion, or gut wall metabolism may contribute considerably to the variable oral bioavailability of etoposide.

In order to determine the effect of the typical CYP3A and P-gp inhibitor on the pharmacokinetics of etoposide, verapamil was administered concomitantly with i.v. and i.g. administered etoposide at doses of 2 and 6 mg/kg to rats. As shown in Table 10, the presence of verapamil caused significantly ($p < 0.01$) slower CL_t, and greater $AUC_{0-\infty}$ of etoposide, which suggests that CYP3A-catalyzed metabolism and P-gp-mediated efflux in the liver and kidney are inhibited, since i.v. administered etoposide is correlated to these

two routes (Lum et al., 1992). Haehner et al. (1996) reported that kidney microsomes contain approximately one hundredth or less of the CYP3A protein detected in liver microsomes, and CYP3A5 is the ubiquitously expressed member of the CYP3A family in renal tissue rather than CYP3A4 of which expressed ubiquitously in hepatic tissue. The kidney contains lower level of CYP3A, but it contains higher level of P-gp than the liver (Fojo et al., 1987b; Gatmaitan and Arias, 1993). So, etoposide is mainly excreted via the liver as metabolites and via kidney as parent form as reported by Relling et al. (1994). Davies and Morris (1993) reported that the blood flow rate in the liver, kidney and gut was 55.2, 36.8 and 30 $ml \cdot min^{-1} \cdot kg^{-1}$, Schuetz et al. (1996) reported the CYP3A4 accounts for 30% of hepatic CYP and 70% of small intestinal CYP (Schuetz et al., 1996). The intestinal metabolism and efflux seems to be of magnitude to the systemic elimination of i.v. administered etoposide. But the liver containes 2- to 5-fold greater amounts of CYP3A protein than enterocytes of the small intestine based on the report of De Waziers et al. (1990), and this difference should be even greater when comparing the total mass of microsomal protein between the intestinal mucosa and liver. Moreover, the intestinal P-gp is lower than kidney. All of these suggests that intestinal metabolism and excretion of i.v. administered etoposide must be considerably lower than the liver and kidney. The presence of verapamil also decreased the CL/F and increased the $AUC_{0-\infty}$ of i.g. administered etoposide significantly (Table 11). F values of etoposide elevated 1.39– to 1.48–fold. The enhanced bioavailability of etoposide suggests that verapamil might be effective to inhibit CYP3A and P-gp in the liver and intestine, specifically in the intestine. Based on the results, concomintant administration of verapamil would be one of the strategies to improve the oral bioavailability of etoposide.

Although verapamil could improve the oral exposure of etoposide, its toxicity would hinder its use in clinical application (Bradshaw and Arceci, 1998). So, this study introduced two flavonoids that were supposed to inhibit P-gp and CYP3A in vitro, quercetin and EGCG, which are abundant in our dietary supplements.

When quercetin at doses of 3, 12 and 20 mg/kg treated 30 min prior to i.v. administration of etoposide, the pharmacokinetic parameters of etoposide have not altered significantly (Table 12). The oral bioavailability of quercetin is prettyl low. Cermak et al., (2003) reported when quercetin at the dose of 50 mg/kg was administered to pigs, the main

metabolites in plasma were always conjugated quercetin, whereas free quercetin was not detected in either the jugular or the portal blood (Cermak et al., 2003). Ader et al., (2000) also reported that the calculated F value of free unchanged quercetin was 0.54 ± 0.19%. The concentration of quercetin in the systemic circulation must be too low to exert its potency on the inhibition of CYP3A and P-gp located in the secretory organs. This assumption could be confirmed by the report of Dupuy et al. (2003) in that coadminstration of 10 mg/kg of quercetin with 0.2 mg/kg of moxidectin subcutaneously significantly increased the AUC of moxidectin, a P-gp and CYP3A substrate, in lamps which might be due to the subcutaneously administered quercetin would not subject to first-pass metabolism as i.g. administration. This result further confirmed the speculation that intestinal metabolism and excretion should be the minor factor to the elimination of i.v. administered etoposide. When etoposide was administered intragastrically, the presence of quercetin significantly reduced the CL/F and increased the $AUC_{0-\infty}$ of etoposide at doses of 3 and 12 mg/kg (Table 13). F value of etoposide elevated by 1.42– to 1.54–fold, which was comparable to that with verapamil (1.39– to 1.48–fold). Cermak et al. (2003) reported in pigs treated with quercetin, the metabolites were found within 1 h with C_{max} gained after 2 h, which indicates that quercetin was absorbed from the small intestine. Manach et al. (1997) also reported that quercetin was easily absorbed in the small intestine in rats. The enhanced oral bioavailability of etoposide might be due to inhibition of P-gp and CYP3A in the intestine. This speculation could be supported by the report of Wang et al. (2004) in that oral coadministration of 40 mg/kg of quercetin with 0.02 mg/kg of digoxin, the substrate of CYP3A and P-gp, in pigs significantly elevated the C_{max} of digoxin by 413% and increased the AUC_{0-t} by 170%. Although quercetin at a dose of 20 mg/kg also increased the AUC and reduced the CL/F of etoposide, they are not significant statistically. Interestingly, this results are consistent with another study in our laboratory (Shin et al., 2006) in which coadministration of tamoxifen with quercetin at doses of 2.5 and 7.5 mg/kg in rats showed the significantly increased AUC and C_{max} of tamoxifen compared to the control group (given tamoxifen alone), but not by coadministration of quercetin at a dose of 15 mg/kg. Hsiu et al. (2002) reported that $AUC_{(0-3)}$ and $AUC_{(0-t)}$ of cyclosporin (10 mg/kg), a substrate for both CYP3A4 and P-gp, decreased significantly by 56% and 43% when quercetin at a dose of 50 mg/kg orally

coadministered to pigs and rats. Orally administered quercetin undergoes extensive Phase I and Phase II metabolism and present in the systemic circulation as a complex mixture of free aglycone with glucuronidated, sulphated and methylated (isorhamnetin, tamarixetin) form. At 20 mg/kg of quercetin, there might be other factors such as the conjugated form of quercetin affects the pharmacokinetics of etoposide since they are substrates for MRPs efflux in vitro (O'Leary et al., 2003), which needs to be investigated further.

As shown in table 14, the presence of 12 mg/kg of EGCG decreased the CL_t and increased the $AUC_{0-\infty}$ of i.v. administered etoposide significantly ($p < 0.05$), which suggests that CYP3A-mediated metabolism and P-gp-mediated efflux of etoposide in the liver and kidney might be inhibited by EGCG as verapamil. These results are consistent with that reported by Carcel-Trullols et al. (2004) in that cyclosporin A as a dual CYP 3A4 and P-gp inhibitor increased the plasma concentration and decreased the plasma clearance of etoposide when infused 1 hour prior to intravenous administration of etoposide in rats, which has also been conformed in patients (Lum et al., 1992). EGCG at a dose of 3 mg/kg also reduced the CL_t and increased the $AUC_{0-\infty}$ of etoposide, but they were not significant. Since the bioavailability of orally administered EGCG is low based on in rat's study (Chen et al., 1997), plasma concentration of EGCG at the dose of 3 mg/kg might be not high enough to inhibit CYP3A enzymatic function or P-gp mediated excretion in the liver and kidney. When etoposide was administered orally, EGCG also decreased the CL/F and increased the $AUC_{0-\infty}$ of etoposide (Table 15). EGCG might be effective in reversing the enteric first-pass extraction of orally administered etoposide since the orally administered EGCG subjects to the intestinal extraction more than hepatic extraction (Chen et al., 1997; Cai et al., 2002), of which contribute to the concentration of EGCG in the enterocytes much higher than in the hepatocytes and the CYP3A and P-gp in the intestine should be inhibited more than that in the liver. EGCG at a dose of 3 mg/kg enhanced the oral bioavailability of etoposide more than 12 mg/kg. Since EGCG and its methyl metabolites are substrates for MRP1 and MRP2 but not P-gp (Hong et al., 2003), MRPs, specifically MRP1, mediated transport of etoposide in the intestine might be influenced by increasing the dose of EGCG. The presence of EGCG enhanced the oral bioavailability of etoposide, which was comlparable with the high dose of veapamil (10 mg/kg).

5. CONCLUSION

Pharmacokientic behavior of etoposide after i.g. (10 mg/kg), i.p. (3.3 mg/kg) and i.v. (3.3 mg/kg) administration in rats was as follows:

(1) F value of etoposide was 0.987 in i.p. route, which indicates that intraportal etoposide would not subject to the hepatic first-pass extraction considerably.

(2) F value of etoposide was 0.084 in i.g. group, approximately 92% of etoposide failed to access the systemic circulation.

The presence of verapamil at doses of 2 and 6 mg/kg significantly altered the pharmacokinetic parameters of i.v. (10 mg/kg) and i.g. (3.3 mg/kg) administered etoposide as follows:

(1) When etoposide was administered intravenously, the CL_t of etoposide was significantly slower ($p < 0.01$, approximately 27.5%) and the $AUC_{0-\infty}$ of etoposide was significantly greater ($p < 0.01$, 37.7%–38.4%) in the presence of verapamil.

(2) When etoposide was administered intragastrically, the CL/F of etoposide was significantly slower ($p < 0.01$, 27.8–31.2%) and the $AUC_{0-\infty}$ of etoposide was significantly greater ($p < 0.05$ at 2 mg/kg, $p < 0.01$ at 6 mg/kg, 39.2–47.6%) in the presence of verapamil.

(3) F value of i.g. administered etoposide elevated 1.39– to 1.48–fold.

When pretreated with quercetin at doses of 3, 12 or 20 mg/kg, the pharmacokinetic parameters of etoposide altered significantly in i.g. group but not in i.v. group.

(1) When etoposide was administered intragastrically, the CL/F of etoposide was significantly slower ($p < 0.01$, 27.6 – 33.7%) and the $AUC_{0-\infty}$ of etoposide was significantly greater ($p < 0.01$, 41.7 – 54.0%) in the presence of quercetin at doses of 3 and 12 mg/kg.

(2) F values of etoposide elevated 1.42– to 1.54– fold, which was comparable with 2 and 6 mg/kg of verapamil.

When pretreated with EGCG at doses of 3, 12 or 20 mg/kg, the pharmacokinetic parameters of etoposide altered significantly both in i.v. and i.g. routes.

(1) When etoposide was administered intravenously, the CL_t of etoposide was

significantly slower ($p < 0.05$, 25.1%), and the $AUC_{0-\infty}$ of etoposide was significantly greater ($p < 0.05$, 33.4%) in the presence of EGCG at a dose of 12 mg/kg, which is comparable with verapamil at doses of 2 and 6 mg/kg.

(2) When etoposide was administered intragastrically, the CL/F of etoposide was significantly slower ($p < 0.01$, 30.5–43.9%), and the $AUC_{0-\infty}$ of etoposide was significantly greater (44.9–81.6%, $p < 0.01$ at 3 and 12 mg/kg, $p < 0.05$ at 20 mg/kg) and C_{max} of etoposide was significantly higher (48.1–80.1%, $p < 0.01$ at 3 mg/kg, $p < 0.05$ at 12 and 20 mg/kg) in the presence of EGCG.

(3) F values of etoposide in the presence of EGCG were 1.52– to 1.81–fold higher than the oral control group, which was comparable with verapamil at the dose of 6 mg/kg.

Enteric first-pass extraction might be the main contributor of the low oral bioavailability of etoposide in rats. The presence of the flavonoids, quercetin and EGCG, enhanced the oral exposure of etoposide, which were as effective as verapamil, a typical P-gp and CYP3A inhibitor, in terms of increase of the absolute bioavailability. Since quercetin and EGCG have many health-promoting benefits and have no consistent side effects, it might be available as the MDR modulators in the clinical therapy to improve the oral bioavailability of etoposide in humans. The dosage regimen of etoposide in anticancer therapy should take into account of these flavonoids or the dietary supplements that full of these flavonoids, specifically when administered orally.

REFERENCES

Ader P, Wessmann A, Wolffram S. Bioavailability and metabolism of the flavonol quercetin in the pig. Free Radic Biol Med 2000; 28: 1056-1067.

Allen LM, Creaven PJ. Comparison of the human pharmacokinetics of VM-26 and VP-16, two antineoplastic epipodophyllotixin glucopyranoside derivatives. Eur J Cancer 1975; 11: 697-707.

Anderle P, Niederer E, Rubas W, Hilgendorf C, Spahn-Langguth H, Wunderli-Allenspach H, Merkle HP, Langguth P. P-glycoprotein (P-gp) mediated efflux in Caco-2 cell monolayers: the influence of culturing conditions and drug exposure on P-gp expression levels, J Pharm Sci 1998; 87: 757-762.

Allen JD, van Dort SC, Buitelaar M, van Tellingen O, Schinkel AH. Mouse breast cancer resistance protein (BCRP1/Abcg2) mediates etoposide resistance and transport, but etoposide oral availability is limited primarily by P-glycoprotein. Cancer Res 2003; 63: 1339-1344.

Bar-Meir S, Halpern Z, Gutman M, Shpirer Z, Baratz M, Bass D. Effect of (+)-cyanidanol-3 on chronic active hepatitis: a double-blind controlled trial. Gut 1985; 26: 975-979.

Bobrowska-Hagerstrand M, Wrobel A, Mrowczynska L, Soderstrom T, Shirataki Y, Motohashi N, Molnar J, Michalak K, Hagerstrand H. Flavonoids as inhibitors of MRP1-like efflux activity in human erythrocytes. A structure–activity relationship study. Oncol Res 2003; 13: 463-469.

Borst P, Kool M, Evers R. Do cMOAT (MRP2), other MRP homologues, and LRP play a role in MDR? Cancer Biol 1997; 8: 205-213.

Bradshaw DM, Arceci RJ. Clinical relevance of transmembrane drug efflux as a mechanism of multidrug resistance. J Clin Oncol 1998; 16: 3674-3690.

Buchler M, Konig J, Brom M, Kartenbeck J, Spring H, Horie T, Keppler D. cDNA cloning of the hepatocyte canalicular isoform of the multidrug resistance protein, cMrp, reveals a novel conjugate export pump deficient in hyperbilirubinemic mutant rats. J Biol Chem 1996; 271: 15091-15098.

Cai Y, Anavy ND, Chow HH. Contribution of presystemic hepatic extraction to the low oral bioavailability of green tea catechins in rats. Drug Metab Dispos 2002; 30: 1246-1249.

Carcel-Trullols J, Torres-Molina F, Araico A, Saadeddin A, Peris JE. Effect of cyclosporine A on the tissue distribution and pharmacokinetics of etoposide, Cancer Chemother. Pharmacol. 54 (2004) 153-160

Castro AF, Altenberg GA. Inhibition of drug transport by genistein in multidrug-resistant cells expressing P-glycoprotein. Biochem Pharmacol 1997; 53: 89-93.

Cermak R, Landgraf S, Wolffram S. The bioavailability of quercetin in pigs depends on the glycoside moiety and on dietary factors. J Nutr 2003; 133: 2802-2807.

Chen L, Lee MJ, Li H, Yang CS. Absorption, distribution, elimination of tea polyphenols in rats. Drug Metab Dispos 1997; 25: 1045-1050.

Cheng ZQ, Radominska-Pandya A, Tephly TR. Studies on the substrate specificity of human intestinal UDP-glucuronosyltransferases 1A8 and 1A10. Drug Metab Dispos 1999; 27: 1165-1170.

Cherrington NJ, Hartley DP, Li N, Johnson DR, Klaassen CD. Organ distribution of multidrug resistance proteins 1, 2, and 3 (Mrp1, 2, and 3) mRNA and hepatic induction of Mrp3 by constitutive androstane receptor activators in rats. J Pharmacol Exp Ther 2002; 300: 97–104.

Chu D-C, Juneja LR. In: Yamamoto T, Juneja LR, Chu D-C, Kim M. (Eds.), Chemistry and Applications of Green Tea, CRC Press, New York, 1997, pp. 13–22.

Clark PI, Slevin ML. The clinical pharmacology of etoposide and teniposide. Clin Pharmacokinet 1987; 12: 223-252.

Conn HO. Cyanidanol: will a hepatotrophic drug from Europe go west? Hepatology 1983; 3: 121–123.

Cooray HC, Janvilisri T, van Veen HW, Hladky SB, Barrand MA. Interaction of the breast cancer resistance protein with plant polyphenols. Biochem Biophys Res Commun 2004; 317: 269-275.

Cordon-Cardo C, O'Brien JP, Casals D, Bertino JR, Melamed MR. Expression of the multidrug resistance gene product (P-glycoprotein) in human normal and tumor tissues. J Histochem Cytochem 1990; 38: 1277–1287.

Crespy V, Morand C, Manach C, Besson C, Demigne C, Remesy C. Part of quercetin absorbed in the small intestine is conjugated and further secreted in the intestinal lumen. Am J Physiol 1999; 277: G120–G126.

Davies B, Morris T. Physiological parameters in laboratory animals and humans. Pharm Res 1993; 10: 1093-1095.

Day AJ, Dupont MS, Ridley S, Rhodes M, Rhodes MJC, Morgan MRA, Williamson G. Deglycosylation of flavonoid and isoflavonoid glycosides by human small intestine and liver ß-glucosidase activity. FEBS Lett 1998; 436: 71-75.

Day AJ, Canada FJ, Diaz JC, Kroon PA, McLauchlan R, Faulds CB, Plumb G, Morgan MRA, Williamson G. Dietary flavonoid and isoflavone glycosides are hydrolysed by the lactase site of lactase phlorizin hydrolase. FEBS Lett 2000; 468: 166–170.

Demant EJ, Sehested M, Jensen PB. A model for computer simulation of P-glycoprotein and transmembrane delta pH-mediated anthracycline transport in multidrug-resistant tumor cells. Biochim Biophys Acta 1990; 1055: 117–125.

Dow LW, Sinkule JA, Look AT, Horvath A, Evans WE. Comparative cytotoxic and cytokinetic effects of the epipodophyllotoxins 4'-demethylepipodo-phyllotoxin-9-(4,6-O-2-ethylidene-beta-D-glucopyranoside) and 4'-demethyl-epipodophyllotoxin-9-(4,6-O-2-thenylidene-beta-D-glucopyranoside) and their metabolites on human leukemic lymphoblasts. Cancer Res 1983; 43: 5699-5706.

Dupuy J, Larrieu G, Sutra JF, Lespine A, Alvinerie M. Enhancement of moxidectin bioavailability in lamb by a natural flavonoid: quercetin. Vet Parasitol 2003; 112: 337-247.

Fan D, Beltran PJ, O'Brien CA. Reversal of multidrug resistance. In: Kellen JA, (Edit), 1994. Reversal of Multidrug Resistance in Cancer. CRC Press, Boca Raton FL 1994; 93–124.

Flens MJ, Zaman GJ, van der Valk P, Izquierdo MA, Schroeijers AB, Scheffer GL, van der Groep P, de Haas M, Meijer CJ, Scheper RJ. Tissue distribution of the multidrug resistance protein. Am J Pathol 1996; 148: 1237-1247.

Fojo AT, Shen DW, Mickley LA, Pastan I, Gottesman MM. Intrinsic drug resistance in human kidney cancer is associated with expression of a human multidrug-resistance gene. J Clin Oncol 1987a; 5: 1922-1927.

Fojo AT, Ueda K, Slamon DJ, Poplack DG, Gottesman MM, Pastan I. Expression of a multidrug-resistance gene in human tumors and tissues. Proc Natl Acad Sci USA 1987b; 84: 265-269.

Ford JM, Hait WN. Pharmacology of drugs that alter multidrug resistance in cancer. Pharmacol Rev 1990; 42: 155-199.

Ford JM, Hait WN. Pharmacologic circumvention of multidrug resistance. Cytotechnology 1993; 12: 171-212.

Fossen T, Pedersen AT, Anderson OM. Flavonoids from red onion (Allium cepa). Phytochemistry 1998; 47: 281-285.

Fromm MF, Kauffman HM. Fritz P, Burk O, Kroemer HK, Warzok RW, Eichelbaum M, Siegmund W, Schrenk D. The effect of rifampin treatment on intestinal expression of human MRP transporters. Am J Pathol 2000; 157: 1575–1580.

Gatmaitan ZC, Arias IM. Structure and function of P-glycoprotein in normal liver and small intestine. Adv Pharmacol 1993; 24: 77-97.

Gee JM, DuPont MS, Day AJ, Plumb GW, Williamson G, Johnson IT. Intestinal transport of quercetin glycosides in rats involves both deglycosylation and interaction with the hexose transport pathway. J Nutr 2000; 130: 2765–2771.

Gottesman MM, Pastan I. Biochemistry of multidrug resistance mediated by the multidrug transporter. Annu Rev Biochem 1993; 62: 385–427.

Graefe EU, Wittig J, Mueller S, Riethling AK, Uehleke B, Drewelow B, Pforte H, Jacobasch G, Derendorf H, Veit M. Pharmacokinetics and bioavailability of quercetin glycosides in humans. J Clin Pharmacol 2001; 41: 492-499.

Grant CE, Valdimarsson G, Hipfner DR, Almquist KC, Cole SP, Deeley RG. Overexpression of multidrug resistance-associated protein increases resistance to natural product drugs. Cancer Res 1994; 54: 357–361.

Griffiths LA, Barrow A. Metabolism of flavonoid compounds in germ-free rats. Biochem J 1972; 130: 1161-1162.

Guengerich FP. Human cytochrome P450 enzymes. In: Ortiz de Montellano P. (Ed.). Cytochrome P450. Plenum Press, New York 1995; 473–535.

Haehner BD, Gorski JC, Vandenbranden M, Wrighton SA, Janardan SK, Watkins PB, Hall SD. Bimodal distribution of renal cytochrome P450 3A activity in humans. Mol

Pharmacol. 1996; 50: 52-59.

Haim N, Nemec J, Roman J, Sinha BK. Peroxidase-catalyzed metabolism of etoposide (VP-16-213) and covalent binding of reactive intermediates to cellular macromolecules. Cancer Res 1987; 47: 5835-5840.

Harrison LI, Gibaldi M. Pharmacokinetics of digoxin in the rat. Drug Metab Dispos 1976; 4: 88-93.

Hayashi M, Tomita M, Awzu S. Transcellular and paracellular contribution to transport processes in the colorectal route. Adv Drug Deliv Rev 1997; 28: 191–204.

Herrmann K. On the occurrence of flavonol and flavone glycosides in vegetables. Z Lebensm Unters Forsch 1988; 186: 1-5.

Hertog MGL, Hollman PCH, Katan MB. Content of potentially anticarcinogenic flavonoids of 28 vegetables and 9 fruits commonly consumed in the Netherlands. J Agric Food Chem 1992; 40: 2379-2383.

Hertog MG, Hollman PC, Katan MB, Kromhout D. Intake of potentially anticarcinogenic flavonoids and their determinants in adults in The Netherlands. Nutr Cancer 1993a; 20: 21-29.

Hertog MG, Feskens EJ, Hollman PC, Katan MB, Kromhout D. Dietary antioxidant flavonoids and risk of coronary heart disease: the Zutphen Elderly Study. Lancet 1993b; 342: 1007-1011.

Hertog MG, Kromhout D, Aravanis C, Blackburn H, Buzina R, Fidanza F, Giampaoli S, Jansen A, Menotti A, Nedeljkovic S, et al. Flavonoid intake and long-term risk of coronary heart disease and cancer in the seven countries study. Arch Intern Med 1995; 155: 381-386. Erratum in: Arch Intern Med 1995; 155: 1184.

Higdon JV, Frei B. Tea catechins and polyphenols: health effects, metabolism, and antioxidant functions. Crit Rev Food Sci Nutr 2003; 43: 89–143.

Ho PC, Saville DJ, Wanwimolruk S. Inhibition of human CYP3A4 activity by grapefruit flavonoids, furanocoumarins and related compounds. J Pharm Pharm Sci 2001; 4: 217-227.

Hodek P, Trefil P, Stiborova M. Flavonoids-potent and versatile biologically active compounds interacting with cytochromes P450. Chem Biol Interact 2002; 139: 1-21.

Hollman PCH, van Trijp JMP, Buysman MNCP, van der Gaag MS, Mengelers MJB, de

Vries JHM, Katan MB. Relative bioavailability of the antioxidant flavonoid quercetin from various foods in man. FEBS Lett 1997; 418: 152-156.

Hollman PCH, Bijsman MNCP, van Gameren Y, Cnossen EPJ, de Vries JHM, Katan MB. The sugar moiety is a major determinant of the absorption of dietary flavonoid glycosides in man. Free Radic Res 1999; 31: 569-573.

Hong J, Lambert JD, Lee SH, Sinko PJ, Yang CS. Involvement of multidrug resistance-associated proteins in regulating cellular levels of (-)-epigallocatechin-3-gallate and its methyl metabolites. Biochem Biophys Res Commun 2003; 310: 222-227.

Hsiu SL, Hou YC, Wang YH, Tsao CW, Su SF, Chao PD. Quercetin significantly decreased cyclosporin oral bioavailability in pigs and rats. Life Sci 2002; 72: 227-235.

Hunter J, Hirst BH. Intestinal secretion of drugs. The role of P-glycoprotein and related drug efflux systems in limiting oral drug absorption. Adv Drug Del Rev 1997; 25: 129-157.

Hyafil F, Vergely C, Du Vignaud P, Grand-Perret T. In vitro and in vivo reversal of multidrug resistance by GF120918, an acridonecarboxamide derivative. Cancer Res 1993; 53: 4595–4602.

Jain RK. Transport of molecules in the tumour interstitium: a review. Cancer Res 1987; 47: 3039-3051.

Jedlitschky G, Leier I, Buchholz U, Hummel-Eisenbeiss J, Burchell B, Keppler D. ATP-dependent transport of bilirubin glucuronides by the multidrug resistance protein MRP1 and its hepatocyte canalicular isoform MRP2. Biochem J 1997; 327: 305-310.

Jodoin J, Demeule M, Beliveau R. Inhibition of the mutldrug resistance P-glycoprotein activity by green tea polyphenols. Biochim. Biophys Acta 2002; 1542: 149-159.

Joel SP, Clark PI, Heap L, Webster L, Robbins S, Craft H, Slevin ML. Pharmacological attempts to improve the bioavailability of oral etoposide. Cancer Chemother Pharmacol 1995; 37: 125-133.

Kawabe T, Chen ZS, Wada M, Uchiumi T, Ono M, Akiyama S, Kuwano M. Enhanced transport of anticancer agents and leukotriene C4 by the human canalicular multispecific organic anion transporter (cMOAT/MRP2). FEBS Lett 1999; 456: 327-331.

Kawashiro T, Yamashita K, Zhao XJ, Koyama E, Tani M, Chiba K, Ishizaki T. A study on the metabolism of etoposide and possible interactions with antitumor or supporting agents by human liver microsomes. J Pharmacol Exp Ther 1998; 286: 1294-1300.

Keli SO, Hertog MGL, Feskens EJM, Kromhout D. Dietary flavonoids, antioxidant vitamins, and incidence of stroke. Arch Intern Med 1996; 156: 637-642.

Keller RP, Altermatt HJ, Donatsch P, Zihlmann H, Laissue JA, Hiestand PC. Pharmacologic interactions between the resistance-modifying cyclosporine SDZ PSC 833 and etoposide (VP 16-213) enhance *in vivo* cytostatic activity and toxicity. Int J Cancer 1992; 51: 433-438,

Keppler D, Cui Y, Konig J, Leier I, Nies A. Export pumps for anionic conjugates encoded by MRP genes. Adv Enzyme Regul 1999;39:237-246.

Kiviranta J, Huovinen K, Hiltunen R. Variation of phenolic substances in onion. Acta Pharm. Fenn 1988; 97: 67-72.

Kiya K, Uozumi T, Ogasawara H, Sugiyama K, Hotta T, Mikami T, Kurisu K. Penetration of etoposide into human malignant brain tumors after intravenous and oral administration. Cancer Chemother Pharmacol 1992; 29: 339-342.

Knasmuller S, Parzefall W, Sanyal R, Ecker S, Schwab C, Uhl M, Mersch-Sundermann V, Williamson G, Hietsch G, Langer T, Darroudi F, Natarajan AT. Use of metabolically competent human hepatoma cells for the detection of mutagens and antimutagens. Mut Res 1998; 402: 185–202.

Knekt P, Jarvinen R, Seppanen R, Hellovaara M, Teppo L, Pukkala E, Aromaa A. Dietary flavonoids and the risk of lung cancer and other malignant neoplasms. Am J Epidemiol 1997;146: 223-230.

Koike K, Kawabe T, Tanaka T, Toh S, Uchiumi T, Wada M, Akiyama S, Ono M, Kuwano M. A canalicular multispecific organic anion transporter (cMOAT) antisense cDNA enhances drug sensitivity in human hepatic cancer cells. Cancer Res 1997; 57: 5475-5479.

Kuroda Y, Hara Y. Antimutagenic and anticarcinogenic activity of tea polyphenols, Mutat Res 1999; 436: 69-97.

Lamson DW, Brignall MS. Antioxidants and cancer, part 3: quercetin. Altern Med Rev 2000; 5: 196-208.

Lee MJ, Maliakal P, Chen L, Meng X, Bondoc FY, Prabhu S, Lambert G, Mohr S, Yang CS. Pharmacokinetics of tea catechins after ingestion of green tea and (-)-epigallocatechin-3-gallate by humans: formation of different metabolites and individual variability. Cancer Epidemiol Biomarkers Prev 2002; 11: 1025-1032.

Lee TK, Hammond CL, Ballatori N. Intracellular glutathione regulates taurocholate transport in HepG2 cells. Toxicol Appl Pharmacol 2001; 174: 207-215.

Leu BL, Huang JD. Inhibition of intestinal P-glycoprotein and effects on etoposide absorption. Cancer Chemother Pharmacol 1995; 35: 432-436.

Liliemark E, Pettersson B, Peterson C, Liliemark J. High-performance liquid chromatography with fluorometric detection for monitoring of etoposide and its cis-isomer in plasma and leukaemic cells. J Chromatogr B Biomed Appl 1995; 669: 311–317.

Lu H, Meng X, Yang CS. Enzymology of methylation of tea catechins and inhibition of catechol-*O*-methyltransferase by (−)-epigallocatechin gallate. Drug Metab Dispos 2003a; 31: 572–579.

Lu H, Meng X, Li C, Sang S, Patten C, Sheng S, Hong J, Bai N, Winnik B, Ho CT, Yang CS. Glucuronides of tea catechins: enzymology of biosynthesis and biological activities. Drug Metab. Dispos 2003b; 31: 452–461.

Lum BL, Kaubisch S, Yahanda AM, Adler KM, Jew L, Ehsan MN, Brophy NA, Halset J, Gosland MP, Sikic B. Alteration of etoposide pharmacokinetics and pharmacodynamics by cyclosporine in a phase I trial to modulate multidrug resistance. J Clin Oncol 1992; 10: 1635-1642.

Luiz da Silva E, Tsushida T, Terao J. Inhibition of mammalian 15-lipoxygenase-dependent lipid peroxidation in low-density lipoprotein by quercetin and quercetin monoglucosides.Arch Biochem Biophys 1998; 349: 313-320.

van Maanen JM, de Vries J, Pappie D, van den Akker E, Lafleur VM, Retel J, van der Greef J, Pinedo HM. Cytochrome P-450-mediated O-demethylation: a route in the metabolic activation of etoposide (VP-16-213). Cancer Res 1987; 47: 4658-4662.

Manach C, Morand C, Demigne C, Texier O, Regerat F, Remesy C. Bioavailability of rutin and quercetin in rats. FEBS Lett 1997; 409: 12-16.

Manouilov KK, McGuire TR, Gordon BG, Gwilt PR. Assay for etoposide in human serum

using solid-phase extraction and high-performance liquid chromatography with fluorescence detection. J Chromatogr B Biomed Sci Appl 1998; 707: 342–346.

Martel F, Grundemann D, Calhau C, Schomig E. Apical uptake of organic cations by human intestinal Caco-2 cells: putative involvement of ASF transporters. Naunyn Schmiedebergs Arch Pharmacol. 2001; 363: 40-49.

Mayer R, Kartenbeck J, Buchler M, Jedlitschky G, Leier I, Keppler D. Expression of the MRP gene-encoded conjugate export pump in liver and its selective absence from the canalicular membrane in transport-deficient mutant hepatocytes. J Cell Biol 1995; 131: 137-150.

McEvoy GK (ed) (2000) AHFS drug information. American Society of Health-System Pharmacists, Bethesda, pp 917–924.

Merkel DE, Fuqua SAW, Tandom AK, Hill SM, Buzdar AU, McGuire WL. Electrophoretic analysis of 248 clinical breast cancer specimens for P-glycoprotein overexpression of gene amplification. J Clin Oncol 1989; 7: 1129-1136.

Mukhtar H, Ahmad N. Tea polyphenols: prevention of cancer and optimizing health. Am J Clin Nutr 2000; 71(suppl.): 1698S-1702S.

Murota K, Terao J. Antioxidative flavonoid quercetin: implication of its intestinal absorption and metabolism. Arch Biochem Biophys 2003; 417: 12-17.

Muto S, Fujita K, Yamazaki Y, Kamataki T. Inhibition by green tea catechins of metabolic activation of procarcinogens by human cytochrome P450. Mutat Res 2001; 479: 197-206.

Ofer M, Wolffram S, Koggel A, Spahn-Langguth H, Langguth P. Modulation of drug transport by selected flavonoids: Involvement of P-gp and OCT? Eur J Pharm Sci 2005; 25: 263-271.

O'Leary KA, Day AJ, Needs PW, Mellon FA, O'Brien NM, Williamson G. Metabolism of quercetin-7- and quercetin-3-glucuronides by an in vitro hepatic model: the role of human beta-glucuronidase, sulfotransferase, catechol-O-methyltransferase and multi-resistant protein 2 (MRP2) in flavonoid metabolism. Biochem Pharmacol 2003; 65: 479-491.

Ozvegy C, Litman T, Szakacs G, Nagy Z, Bates S, Varadi A, Sarkadi B. Functional characterization of the human multidrug transporter, ABCG2, expressed in insect

cells. Biochem Biophys Res Commun 2001; 285: 111-117.

Pastan I, Gottesman MM. Multidrug resistance. Ann Rev Med 1991; 42: 277-286.

Patel J, Buddha B, Dey S, Pal D, Mitra AK. In vitro interaction of the HIV protease inhibitor ritonavir with herbal constituents: changes in P-gp and CYP3A4 activity. Am J Ther 2004; 11: 262-277.

Peng KC, Cluzeaud F, Bens M, van Huyen JP, Wioland MA, Lacave R, Vandewalle A. Tissue and cell distribution of the multidrug resistance-associated protein (MRP) in mouse intestine and kidney. J Histochem Cytochem 1999; 47: 757–768.

Piskula MK, Terao J. Accumulation of (-)-epicatechin metabolites in rat plasma after oral administration and distribution of conjugation enzymes in rat tissues. J Nutr 1998; 128: 1172-1178.

Price KR, Rhodes MJC. Analysis of the major flavonol glycosides present in four varieties of onion (Allium cepa) and changes in composition resulting from autolysis. J Sci Food Agric 1997; 74: 331-339.

Price KR, Bacon JR, Rhodes MJC. Effect of storage and domestic processing on the content and composition of flavonol glucosides in onions (Allium cepa). J Agric Food Chem 1997; 45: 938-942.

Qian F, Wei D, Zhang Q, Yang S. Modulation of P-glycoprotein function and reversal of multidrug resistance by (-)-epigallocatechin gallate in human cancer cells. Biomed Pharmacother 2005; 59: 64-69.

Reif S, Kingreen D, Kloft C, Grimm J, Siegert W, Schunack W, Jaehde U. Bioequivalence investigation of high-dose etoposide and etoposide phosphate in lymphoma patients. Cancer Chemother Pharmacol 2001; 48: 134-140.

Relling MV, Evans R, Dass C, Desiderio DM, Nemec J. Human cytochrome P450 metabolism of teniposide and etoposide. J Pharmacol Exp Ther 1992; 261: 491-496.

Relling MV, Nemec J, Schuetz EG, Schuetz JD, Gonzalez FJ, Korzekwa KR. O-demethylation of epipodophyllotoxins is catalyzed by human cytochrome P450 3A4. Mol Pharmacol 1994; 45: 352-358.

Rimm E B, Katan MB, Ascherio A, Stampfer MJ, Willett WC. Relation between intake of flavonoids and risk for coronary heart disease in male health professionals. Ann Intern Med 1996; 125: 384-389.

Roelofsen H, Vos TA, Schippers IJ, Kuipers F, Koning H, Moshage H, Jansen PL, Muller M. Increased levels of the multidrug resistance protein in lateral membranes of proliferating hepatocyte-derived cells. Gastroenterology 1997; 112: 511-521.

Ross JA, Kasum CM. Dietary flavonoids: bioavailability, metabolic effects, and safety. Annu Rev Nutr 2002; 22: 19-34.

Sakakibara H, Honda Y, Nakagawa S, Ashida H, Kanazawa K. Simultaneous determination of all polyphenols in vegetables, fruits, and teas. J Agric Food Chem 2003; 51: 571-581.

Salphati L, Benet LZ. Metabolism of digoxin and digoxigenin digitoxosides in rat liver microsomes, involvement of cytochrome P_{450} 3A. Xenobiotica 1999; 29: 171–185.

Scambia G, Ranelletti FO, Panici PB, De Vincenzo, R. Bonanno G. and Ferrandina, G. *et al.* Quercetin potentiates the effect of adriamycin in a multidrug-resistant MCF-7 human breast-cancer cell line: P-glycoprotein as a possible target. Cancer Chemother Pharmacol 1994; 34: 459–464.

Schaub TP, Kartenbeck J, Konig J, Spring H, Dorsam J, Staehler G, Storkel S, Thon WF, Keppler D. Expression of the MRP2 gene-encoded conjugate export pump in human kidney proximal tubules and in renal cell carcinoma. J Am Soc Nephrol 1999; 10: 1159-1169.

Schuetz EG, Beck WT, Schuetz JD. Modulators and substrates of P-glycoprotein and cytochrome P4503A coordinately up-regulate these proteins in human colon carcinoma cells. Mol Pharmacol 1996; 49: 311–318.

Sevick EM, Jain RK. Geometric resistance to blood flow in solid tumors perfused ex vivo: effects of tumor size and perfusion pressure. Cancer Res 1989; 49: 3506-3512.

Shin SC, Choi JS, Li X. Enhanced bioavailability of tamoxifen after oral administration of tamoxifen with quercetin in rats. Int J Pharm 2006; 313: 144-149.

Shirazi FH, Bahrami G, Stewart DJ, Tomiak E, Delorme F, Noel D, Goel R. A rapid reversed phase high performance liquid chromatographic method for determination of etoposide (VP-16) in human plasma. J Pharm Biomed Anal 2001;25: 353-356.

Spencer JP, Chowrimootoo G, Choudhury R, Debnam ES, Srai SK, Rice-Evans CA. The small intestine can both absorb and glucuronidate luminal flavonoids. FEBS Lett 1999; 458: 224-230.

Spencer JP, Schroeter H, Crossthwaithe AJ, Kuhnle G, Williams RJ, Rice-Evans C. Contrasting influences of glucuronidation and O-methylation of epicatechin on hydrogen peroxide-induced cell death in neurons and fibroblasts. Free Radic Biol Med 2001; 31: 1139-1146.

Stahelin HF, von Wartburg A. The chemical and biological route from podophyllotoxin glucoside to etoposide: Ninth Cain memorial award lecture. Cancer Res 1991; 51: 5-15

Sutherland L, Ebner T, Burchell B. The expression of UDP-glucuronosyltransferases of the UGT1 family in human liver and kidney and in response to drugs. Biochem Pharmacol 1993; 45: 295-301.

Taipalensuu J, Tornblom H, Lindberg G, Einarsson C, Sjoqvist F, Melhus H, Garberg P, Sjostrom B, Lundgren B, Artursson P. Correlation of gene expression of ten drug efflux proteins of the ATP-binding cassette transporter family in normal human jejunum and in human intestinal epithelial Caco-2 cell monolayers. J Pharmacol Exp Ther 2001; 299: 164-170.

Thiebaut F, Tsuruo T, Hamada H, Gottesman MM, Pastan I, Willingham MC. Cellular localisation of the multidrug-resistance gene product P-glycoprotein in normal human tissues. Proc Natl Acad Sci USA 1987; 84: 7735-7738.

Tsyrlov IB, Mikhailenko VM, Gelboin HV. Isozyme- and species-specific susceptibility of cDNA-expressed CYP1A P-450s to different flavonoids. Biochim Biophys Acta 1994; 1205: 325-335.

Turgeon D, Carrier JS, Levesque E, Hum DW, Belanger A. Relative enzymatic activity, protein stability, and tissue distribution of human steroid-metabolizing UGT2B subfamily members. Endocrinology 2001; 142: 778–787.

Wacher VJ, Wu CY, Benet LZ. Overlapping substrate specificities and tissue distribution of cytochrome P450 3A and P-glycoprotein: implications for drug delivery and activity in cancer chemotherapy. Mol Carcinog 1995; 13: 129-134.

Walle UK, French KL, Walgren RA, Walle T. Transport of genistein-7-glucoside by human intestinal CACO-2 cells: potential role for MRP2. Res Commun Mol Pathol Pharmacol 1999a; 103: 45–56.

Walle UK, Galijatovic A, Walle T. Transport of the flavonoid chrysin and its conjugated

metabolites by the human intestinal cell line Caco-2. Biochem Pharmacol 1999b; 58: 431–438.

Walle T, Eaton EA, Walle UK. Quercetin, a potent and specific inhibitor of the human P-form phenolsulfotransferase. Biochem Pharmacol 1995; 50: 731-734.

Wang YH, Chao PD, Hsiu SL, Wen KC, Hou YC. Lethal quercetin-digoxin interaction in pigs. Life Sci 2004; 74: 1191-1197.

Watkins PB. Drug metabolism by cytochromes P450 in the liver and small bowel. Gastrointest Pharmacol 1992; 21: 511–526.

de Waziers I, Cugnenc PH, Yang CS, Leroux JP, Beaune PH. Cytochrome P 450 isoenzymes, epoxide hydrolase and glutathione transferases in rat and human hepatic and extrahepatic tissues. J Pharmacol Exp Ther 1990; 253: 387-394.

Wozniak AJ, Ross WE. DNA damage as a basis for 4'-demethylepipodophyllotoxin-9-(4,6-O-ethylidene-beta-D-glucopyranoside) (etoposide) cytotoxicity. Cancer Res 1983; 43: 120-124.

Xie J, Li Y, Wang P. Determination of etoposide (VP16) in human serum by high performance liquid chromatography.Se Pu 1998; 16: 74-75.

Zaman GJ, Versantvoort CH, Smit JJ, Eijdems EW, De Haas M, Smith AJ, Broxterman HJ, Mulder NH, De Vries EG, Baas F. Analysis of the expression of MRP, the gene for a new putative transmembrane drug transporter, in human multidrug resistant lung cancer cell lines. Cancer Res 1993; 53: 1747-1750.

van Zanden JJ, Wortelboer HM, Bijlsma S, Punt A, Usta M, Bladeren PJ, Rietjens IM, Cnubben NH. Quantitative structure activity relationship studies on the flavonoid mediated inhibition of multidrug resistance proteins 1 and 2. Biochem Pharmacol 2005; 69: 699-708.

Zhang Q, Wei D, Liu J. In vivo reversal of doxorubicin resistance by (-)-epigallocatechin gallate in a solid human carcinoma xenograft. Cancer Lett 2004; 208: 179-186.

Zhang S, Morris ME. Effects of the flavonoids biochanin A, morin, phloretin, and silymarin on P-glycoprotein-mediated transport. J Pharmacol Exp Ther 2003a; 304: 1258–1267.

Zhang S, Morris ME. Effect of the flavonoids biochanin A and silymarin on the P-glycoprotein-mediated transport of digoxin and vinblastine in human intestinal

Caco-2 cells. Pharm Res 2003b; 20: 1184–1191.

Table 1. Recovery of etoposide and podophyllotoxin from rat's plasma

Concentration (ng/ml)	Peak area (Mean±S.D., n=5)		Recovery (%)
	Extracted	Unextracted	
Etoposide			
50	12831±1671	16028±1439	80.1
200	146864±12510	177328±10787	82.8
1000	614417±38882	739601±26040	83.1
Podophyllotoxin			
2.5	133883±11928	162857±10963	82.2

Table 2. Precision and accuracy of HPLC assay for etoposide from rat plasma

Spiked concentration (ng/ml)	Calculated concentration (ng/ml, mean ± S.D., n = 5)	RSD (%)	Deviation (%)
Intra-day (n = 5)			
10	9.5 ± 1.0	10.5	–4.7
20	17.7 ± 1.8	10.2	–11.5
50	45.7 ± 4.3	9.4	–8.7
100	96.0 ± 9.4	9.8	–4.0
200	199.2 ± 8.9	4.5	–0.4
500	491.1 ± 21.9	4.5	–1.8
1,000	1021.3 ± 50.3	4.9	2.1
2,000	2076.9 ± 32.8	1.6	3.8
Inter-day (n = 5)			
10	9.6 ± 1.1	11.5	–4.0
20	17.3 ± 1.6	9.1	–13.4
50	44.4 ± 5.0	11.2	–11.3
100	91.2 ± 9.9	10.9	–8.8
200	192.7 ± 17.4	9.0	–3.7
500	486.2 ± 19.5	4.0	–2.8
1,000	999.5 ± 61.7	6.2	0.0
2,000	2013.5 ± 103.4	5.1	0.7

Table 3. Mean (+ S.D.) plasma concentration of etoposide after administration of etoposide through intravenous (3.3 mg/kg), intraportal (3.3 mg/kg) and intragastric (10 mg/kg) routes to rats (n = 6, each).

Time (hour)	i.g.	i.p.	i.v.
0.017	–	–	26138.6 ± 3926.4
0.1	204.3 ± 58.7	3673.0 ± 846.3	6425.8 ± 991.6
0.25	367.9 ± 48.2	6107.6 ± 869.2	3655.2 ± 704.4
0.5	470.8 ± 90.9	2531.0 ± 539.5	2189.6 ± 363.7
0.75	449.7 ± 75.7	1419.2 ± 199.6	1283.1 ± 207.4
1	382.4 ± 45.2	1123.0 ± 153.6	901.5 ± 201.8
2	183.2 ± 42.5	537.9 ± 59.8	260.4 ± 77.4
4	79.7 ± 17.9	151.4 ± 33.8	60.9 ± 15.4
6	42.2 ± 12.4	54.2 ± 8.09	25.6 ± 6.7
8	26.2 ± 7.2	27.5 ± 4.91	13.2 ± 3.6
10	17.4 ± 5.1	21.4 ± 3.96	

Table 4. Mean (+ S.D.) plasma concentration of etoposide after intravenous administration at a dose of 3.3 mg/kg in the presence or absence of verapamil at doses of 2 or 6 mg/kg to rats (n = 6, each).

Time (hour)	Control	Etoposide + Verapamil	
		2 mg/kg	6 mg/kg
0.017	26138.6 ± 3926.4	32816.5 ± 3803.9	33450.3 ± 4434.0
0.1	6425.8 ± 991.6	8680.2 ± 1127.4	8657.0 ± 1128.8
0.25	3655.2 ± 704.4	5131.0 ± 546.9	4866.3 ± 771.4
0.5	2189.6 ± 363.7	2967.9 ± 398.1	2837.2 ± 492.1
0.75	1283.1 ± 207.4	1989.4 ± 348.8	1930.3 ± 383.3
1	901.5 ± 201.8	1345.3 ± 320.2	1272.7 ± 226.5
2	260.4 ± 77.4	409.2 ± 105.7	445.4 ± 113.5
4	60.9 ± 15.4	70.6 ± 21.0	92.9 ± 26.7
6	25.6 ± 6.66	30.9 ± 6.09	42.8 ± 11.2
8	13.2 ± 3.61	17.8 ± 5.08	25.0 ± 7.30

Table 5. Mean (+ S.D.) plasma concentration of etoposide after intragastric administration at a dose of 10 mg/kg in the presence or absence of verapamil at doses of 2 or 6 mg/kg in rats (n = 6, each).

Time (hour)	Control	Etoposide + Verapamil	
		2 mg/kg	6 mg/kg
0.0	0	0	0
0.1	204.3 ± 58.7	239.3 ± 52.9	334.8 ± 83.6
0.25	367.9 ± 48.2	409.8 ± 112.8	571.4 ± 87.4
0.5	470.8 ± 90.9	544.9 ± 113.1	667.8 ± 113.2
0.75	449.7 ± 75.7	540.2 ± 107.9	659.1 ± 159.1
1.0	382.4 ± 45.2	477.9 ± 103.2	574.7 ± 162.7
2.0	183.2 ± 42.5	232.0 ± 49.2	231.8 ± 57.0
4.0	79.7 ± 17.9	120.6 ± 26.1	112.1 ± 28.1
6.0	42.2 ± 12.4	76.8 ± 20.2	69.8 ± 17.7
8.0	26.2 ± 7.24	49.4 ± 12.9	45.0 ± 10.5
10.0	17.4 ± 5.12	32.5 ± 9.06	28.9 ± 8.31

Table 6. Mean (+ S.D.) plasma concentration of etoposide after intravenous administration of etoposide at a dose of 3.3 mg/kg in the presence or absence of quercetin at doses of 3, 12 or 20 mg/kg to rats (n = 6, each).

Time (hour)	Control	Etoposide + Quercetin		
		3 mg/kg	12 mg/kg	20 mg/kg
0.017	26138.6 ± 3926.4	28556.6 ± 1529.9	25617.3 ± 2488.3	24277.1 ± 2488.3
0.1	6425.8 ± 991.6	6819.9 ± 730.4	6280.9 ± 779.5	6347.1 ± 779.5
0.25	3655.2 ± 704.4	3760.8 ± 452.5	3613.2 ± 468.8	3756.6 ± 468.8
0.5	2189.6 ± 363.7	2290.5 ± 353.0	2219.5 ± 235.9	2312.0 ± 235.9
0.75	1283.1 ± 207.4	1492.5 ± 283.8	1494.3 ± 227.6	1581.2 ± 227.6
1	901.5 ± 201.8	1094.8 ± 262.4	1099.5 ± 156.6	1094.6 ± 156.6
2	260.4 ± 77.4	359.7 ± 98.3	359.8 ± 75.8	356.4 ± 75.8
4	60.9 ± 15.4	73.7 ± 21.2	92.8 ± 20.6	95.0 ± 20.6
6	25.6 ± 6.66	31.4 ± 8.75	40.1 ± 10.2	40.3 ± 10.2
8	13.2 ± 3.61	17.3 ± 4.95	22.2 ± 5.91	21.0 ± 5.91

Table 7. Mean (+ S.D.) plasma concentration of etoposide after intragastric administration of etoposide at a dose of 10 mg/kg in the presence or absence of quercetin at doses of 3, 12 or 20 mg/kg to rats (n = 6, each).

Time (hour)	Control	Etoposide + Quercetin		
		3 mg/kg	12 mg/kg	20 mg/kg
0	0	0	0	0
0.1	204.3 ± 58.7	241.7 ± 57.2	282.4 ± 80.8	195.6 ± 62.1
0.25	367.9 ± 48.2	403.5 ± 73.2	470.5 ± 132.6	362.9 ± 87.5
0.5	470.8 ± 90.9	522.4 ± 115.5	602.6 ± 118.4	432.7 ± 90.6
0.75	449.7 ± 75.7	569.8 ± 149.6	650.8 ± 101.5	451.6 ± 78.4
1.0	382.4 ± 45.2	546.5 ± 157.6	595.8 ± 74.5	425.0 ± 74.4
2.0	183.2 ± 42.5	321.9 ± 91.9	322.8 ± 74.4	241.6 ± 58.3
4.0	79.7 ± 17.9	101.6 ± 27.8	109.7 ± 24.7	89.8 ± 15.3
6.0	42.2 ± 12.4	55.7 ± 11.7	61.2 ± 16.0	51.1 ± 11.9
8.0	26.2 ± 7.24	35.6 ± 7.49	42.3 ± 11.4	31.9 ± 8.06
10.0	17.4 ± 5.12	26.0 ± 5.89	28.9 ± 8.04	23.1 ± 6.27

Table 8. Mean (+ S.D.) plasma concentration of etoposide after intravenous administration of etoposide at a dose of 3.3 mg/kg in the presence or absence of EGCG at doses of 3 and 12 mg/kg to rats (n = 6, each).

Time (hour)	Control	Etoposide + EGCG	
		3 mg/kg	12 mg/kg
0.017	26138.6 ± 3926.4	28650.6 ± 2577.0	30987.1 ± 2931.8
0.1	6425.8 ± 991.6	7007.1 ± 1365.9	7629.8 ± 715.9
0.25	3655.2 ± 704.4	4068.1 ± 901.9	4516.8 ± 821.0
0.5	2189.6 ± 363.7	2336.9 ± 520.5	2756.9 ± 474.2
0.75	1283.1 ± 207.4	1484.9 ± 428.5	1898.1 ± 408.5
1	901.5 ± 201.8	1003.7 ± 204.6	1412.5 ± 289.4
2	260.4 ± 77.4	365.3 ± 79.3	478.8 ± 108.2
4	60.9 ± 15.4	67.0 ± 18.5	86.3 ± 21.1
6	25.6 ± 6.66	28.8 ± 7.91	38.5 ± 9.63
8	13.2 ± 3.61	15.7 ± 4.52	21.8 ± 6.51

Table 9. Mean (+ S.D.) plasma concentration of etoposide after intragastric administration at a dose of 10 mg/kg in the presence or absence of EGCG at doses of 3, 12 or 20 mg/kg to rats (n = 6, each).

Time (hour)	Control	Etoposide + EGCG		
		3 mg/kg	12 mg/kg	20 mg/kg
0	0	0	0	0
0.1	204.3 ± 58.7	404.4 ± 118.6	396.9 ± 113.8	291.0 ± 76.0
0.25	367.9 ± 48.2	636.4 ± 181.9	559.0 ± 141.3	479.7 ± 138.5
0.50	470.8 ± 90.9	783.8 ± 224.6	684.6 ± 84.4	612.9 ± 163.5
0.75	449.7 ± 75.7	852.3 ± 239.7	622.4 ± 95.4	655.9 ± 125.5
1	382.4 ± 45.2	757.5 ± 196.5	576.3 ± 113.5	585.7 ± 106.4
2	183.2 ± 42.5	351.9 ± 104.6	301.5 ± 58.5	285.6 ± 51.0
4	79.7 ± 17.9	117.3 ± 25.4	107.3 ± 20.3	103.4 ± 25.6
6	42.2 ± 12.4	64.8 ± 19.3	61.2 ± 12.7	53.9 ± 11.9
8	26.2 ± 7.24	42.1 ± 12.2	37.6 ± 5.97	36.4 ± 9.56
10	17.4 ± 5.12	32.8 ± 9.53	28.9 ± 6.15	26.2 ± 7.01

Table 10. Mean (+ S.D.) pharmacokinetic parameters of etoposide after intravenous administration of etoposide at a dose of 3.3 mg/kg in the presence or absence of verapamil at doses of 2 and 6 mg/kg to rats (n = 6, each).

Parameter	Control	Etoposide + Verapamil	
		2 mg/kg	6 mg/kg
$AUC_{0\sim\infty}$ ($ng \cdot h \cdot ml^{-1}$)	4830 ± 754	6652 ± 908**	6683 ± 1025**
K_{el} (h^{-1})	0.382 ± 0.034	0.344 ± 0.091	0.328 ± 0.025
$t_{1/2}$ (h)	1.83 ± 0.169	2.16 ± 0.691	2.12 ± 0.160
CL_t ($ml \cdot min^{-1} \cdot kg^{-1}$)	11.6 ± 1.56	8.40 ± 1.16**	8.41 ± 1.43**
MRT (h)	0.706 ± 0.072	0.747 ± 0.076	0.820 ± 0.069
V_{dss} (L/kg)	0.490 ± 0.078	0.377 ± 0.072	0.410 ± 0.043

* $p < 0.05$, ** $p < 0.01$ compared to control.

$AUC_{0\sim\infty}$: area under the plasma concentration-time curve from 0 h to infinity;

K_{el}: elimination rate constant;

$t_{1/2}$: terminal half-life;

CL_t: total clearance;

MRT: mean residence time;

V_{dss}: volume of distribution at the steady state.

Table 11. Mean (+ S.D.) pharmacokinetic parameters of etoposide after intragastric administration of etoposide at a dose of 10 mg/kg in the presence or absence of verapamil at doses of 2 and 6 mg/kg to rats (n = 6, each).

Parameter	Control	Etoposide +Verapamil	
		2 mg/kg	6 mg/kg
$AUC_{0\sim\infty}$ ($ng \cdot h \cdot ml^{-1}$)	1226 ± 154	1706 ± 235*	1809 ± 347**
C_{max} (ng/ml)	484 ± 74.7	566 ± 102	704 ± 131**
T_{max} (h)	0.500 ± 0.158	0.625 ± 0.137	0.583 ± 0.129
K_{el} (h^{-1})	0.255 ± 0.031	0.220 ± 0.019	0.226 ± 0.029
$t_{1/2}$ (h)	2.75 ± 0.323	3.16 ± 0.264	3.11 ± 0.440
CL/F ($ml \cdot min^{-1} \cdot kg^{-1}$)	137.7 ± 17.8	99.5 ± 16.4**	94.9 ± 17.4**
F	0.084	0.117	0.124

* $p < 0.05$, ** $p < 0.01$ compared to control.

$AUC_{0\sim\infty}$: area under the plasma concentration-time curve from 0 h to infinity;

C_{max}: peak plasma concentration;

T_{max}: time to reach peak plasma concentration;

K_{el}: elimination rate constant;

$t_{1/2}$: terminal half-life;

CL/F: total clearance;

F: absolute bioavailability.

Table 12. Mean (+ S.D.) pharmacokinetic parameters of etoposide after intravenous administration of etoposide at a dose of 3.3 mg/kg in the presence or absence of quercetin at doses of 3, 12 or 20 mg/kg to rats (n = 6, each).

Parameter	Control	Etoposide + Quercetin		
		3 mg/kg	12 mg/kg	20 mg/kg
$AUC_{0\sim\infty}$ ($ng \cdot h \cdot ml^{-1}$)	4830 ± 754	5420 ± 742	5242 ± 838	5245 ± 503
K_{el} (h^{-1})	0.382 ± 0.034	0.362 ± 0.030	0.359 ± 0.037	0.381 ± 0.050
$t_{1/2}$ (h)	1.83 ± 0.169	1.93 ± 0.152	1.95 ± 0.215	1.85 ± 0.248
CL_t ($ml \cdot min^{-1} \cdot kg^{-1}$)	11.6 ± 1.56	10.3 ± 1.40	10.7 ± 1.80	10.6 ± 0.950
MRT (h)	0.706 ± 0.072	0.775 ± 0.082	0.891 ± 0.124	0.888 ± 0.118
V_{dss} (L/kg)	0.490 ± 0.078	0.474 ± 0.026	0.571 ± 0.108	0.563 ± 0.090

* $p < 0.05$ compared to control.

$AUC_{0\sim\infty}$: area under the plasma concentration-time curve from 0 h to infinity;

K_{el}: elimination rate constant;

$t_{1/2}$: terminal half-life;

CL_t: total clearance;

MRT: mean residence time;

V_{dss}: volume of distribution at the steady state.

Table 13. Mean (+ S.D.) pharmacokinetic parameters of etoposide after intragastric administration of etoposide at a dose of 10 mg/kg in the presence or absence of quercetin at doses of 3, 12 or 20 mg/kg to rats (n = 6, each).

Parameter	control	Etoposide + Quercetin		
		3 mg/kg	12 mg/kg	20 mg/kg
$AUC_{0\sim\infty}$ ($ng \cdot h \cdot ml^{-1}$)	1226 ± 154	1737 ± 365*	1888 ± 364**	1419 ± 222
C_{max} (ng/ml)	484 ± 74.7	586 ± 144	673 ± 93.3*	455 ± 80.5
T_{max} (h)	0.500 ± 0.158	0.833 ± 0.204	0.708 ± 0.188	0.667 ± 0.129
K_{el} (h^{-1})	0.255 ± 0.031	0.225 ± 0.025	0.221 ± 0.018	0.230 ± 0.027
$t_{1/2}$ (h)	2.75 ± 0.323	3.11 ± 0.370	3.16 ± 0.282	3.05 ± 0.377
CL/F ($ml \cdot min^{-1} \cdot kg^{-1}$)	137.7 ± 17.8	99.7 ± 21.5**	91.3 ± 19.4**	119.6 ± 16.5
F	0.084	0.119	0.129	0.097

* $p < 0.05$, ** $p < 0.01$ compared to control.

$AUC_{0\sim\infty}$: area under the plasma concentration-time curve from 0 h to infinity;

C_{max}: peak plasma concentration;

T_{max}: time to reach peak plasma concentration;

K_{el}: elimination rate constant;

$t_{1/2}$: terminal half-life;

CL/F: total clearance;

F: absolute bioavailability.

Table 14. Mean (+ S.D.) pharmacokinetic parameters of etoposide after intravenous administration of etoposide at a dose of 3.3 mg/kg in the presence or absence of EGCG at doses of 3 and 12 mg/kg to rats (n = 6, each).

Parameter	control	Etoposide + EGCG	
		3 mg/kg	12 mg/kg
$AUC_{0\sim\infty}$ ($ng \cdot h \cdot ml^{-1}$)	4830 ± 754	5445 ± 958	6444 ± 899*
K_{el} (h^{-1})	0.382 ± 0.034	0.364 ± 0.049	0.349 ± 0.058
$t_{1/2}$ (h)	1.83 ± 0.169	1.93 ± 0.240	2.04 ± 0.384
CL_t ($ml \cdot min^{-1} \cdot kg^{-1}$)	11.6 ± 1.56	10.4 ± 1.86	8.69 ± 1.31*
MRT (h)	0.706 ± 0.072	0.750 ± 0.063	0.833 ± 0.076
V_{dss} (L/kg)	0.490 ± 0.078	0.467 ± 0.096	0.429 ± 0.029

* $p < 0.05$ compared to control.

$AUC_{0\sim\infty}$: area under the plasma concentration-time curve from 0 h to infinity;

K_{el}: elimination rate constant;

$t_{1/2}$: terminal half-life;

CL_t: total clearance;

MRT: mean residence time;

V_{dss}: volume of distribution at the steady state.

Table 15. Mean (+ S.D.) pharmacokinetic parameters of etoposide after intragastric administration of etoposide at a dose of 10 mg/kg in the presence or absence of EGCG at doses of 3, 12 or 20 mg/kg to rats (n = 6, each).

Parameter	Control	Etoposide + EGCG		
		3 mg/kg	12 mg/kg	20mg/kg
$AUC_{0\sim\infty}$ ($ng \cdot h \cdot ml^{-1}$)	1226 ± 154	2227 ± 467**	1874 ± 212**	1776 ± 264*
C_{max} (ng/ml)	484 ± 74.7	872 ± 231**	734 ± 45.4*	717 ± 120*
T_{max} (h)	0.500 ± 0.158	0.750 ± 0.158	0.500 ± 0.274	0.708 ± 0.188
K_{el} (h^{-1})	0.255 ± 0.031	0.215 ± 0.031	0.221 ± 0.021	0.227 ± 0.028
$t_{1/2}$ (h)	2.75 ± 0.323	3.28 ± 0.425	3.16 ± 0.302	3.09 ± 0.374
CL/F ($ml \cdot min^{-1} \cdot kg^{-1}$)	137.7 ± 17.8	77.3 ± 14.4**	89.9 ± 10.4**	95.7 ± 14.9**
F	0.084	0.152	0.128	0.121

* $p < 0.05$, ** $p < 0.01$ compared to control.

$AUC_{0\sim\infty}$: area under the plasma concentration-time curve from 0 h to infinity;

C_{max}: peak plasma concentration;

T_{max}: time to reach peak plasma concentration;

K_{el}: elimination rate constant;

$t_{1/2}$: terminal half-life;

CL/F: total clearance;

F: absolute bioavailability.

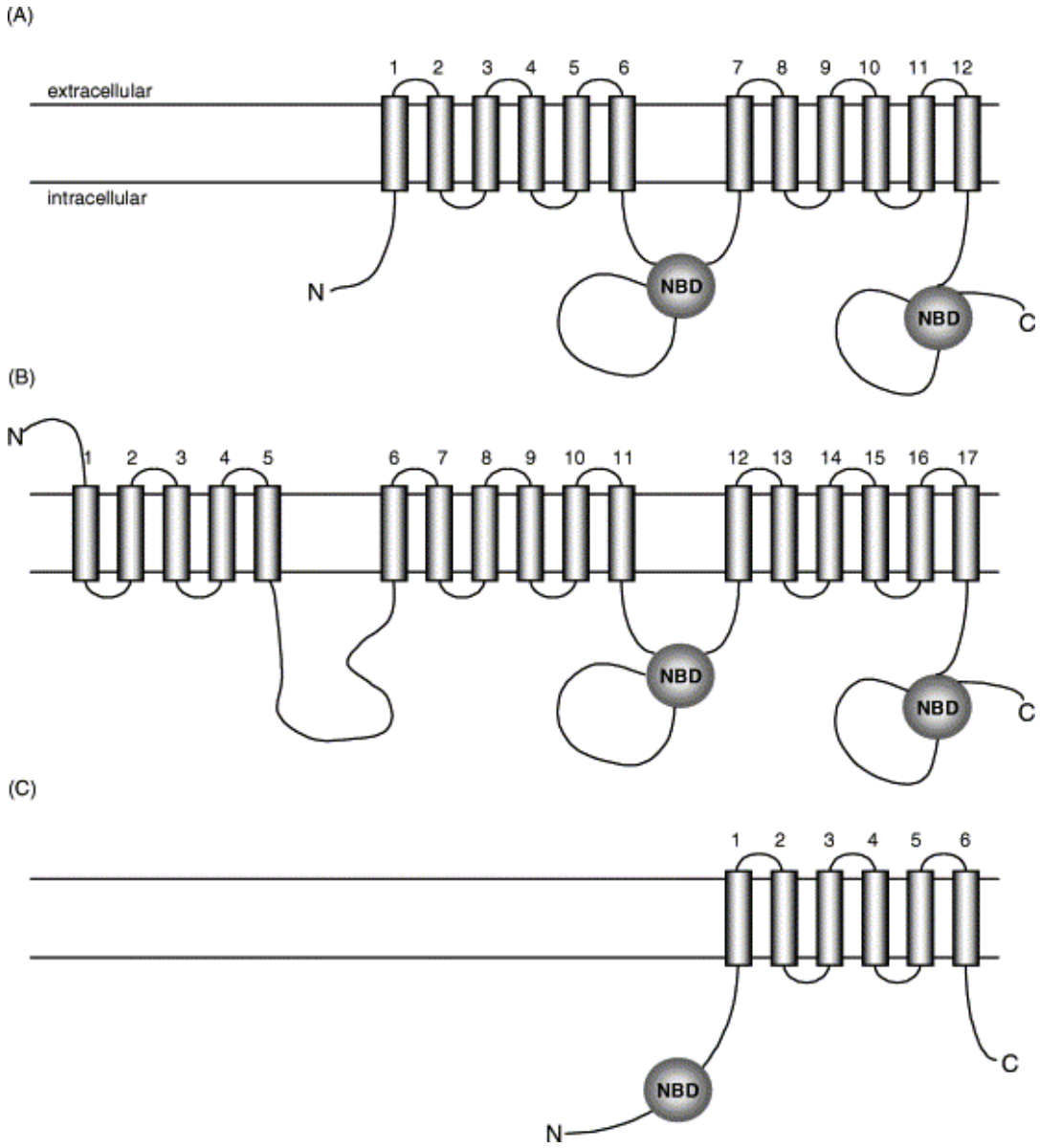

Figure 1. Transmembrane arrangement of ABC efflux proteins. (A) Pgp (MDR1), MDR3, BSEP (SPgp), MRP4, MRP5, and MRP8, have 12 TM (transmembrane) regions and two NBDs (nucleotide binding domains). (B) Typical MRP transporters (MRP1-3 and 6–7) have five extra TM regions towards the N terminus. (C) 'Half-transporters' such as BCRP have just six TM regions and one NBD (Cited from Chan et al., 2004).

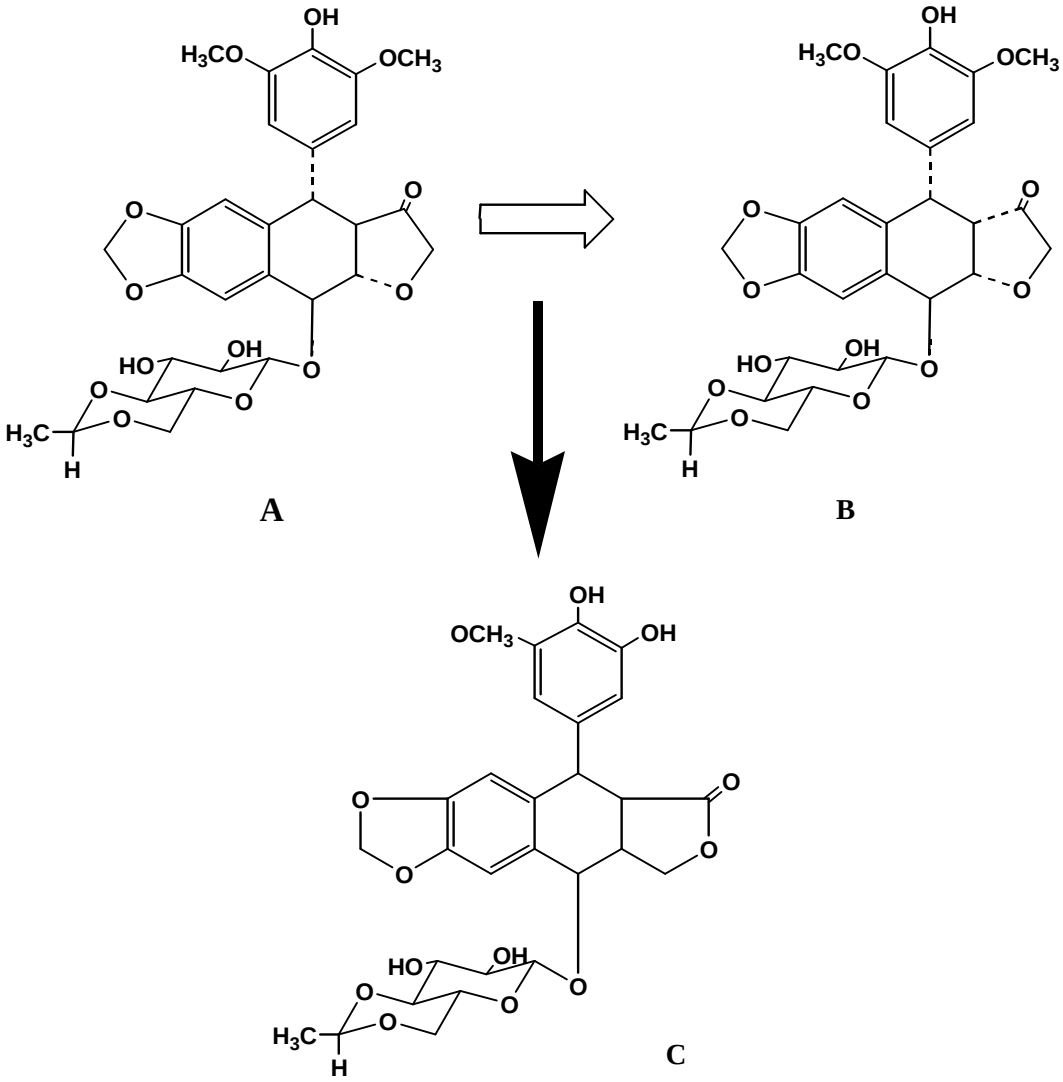

Figure 2. Chemical structure of trans-lactone (A) of etoposide and its degraded pharmacologically inactive isomer cis-lactone form (B) which produced in neutral, weak acidic and alkaline conditions, and the phase I metabolite, etoposide catechol (C).

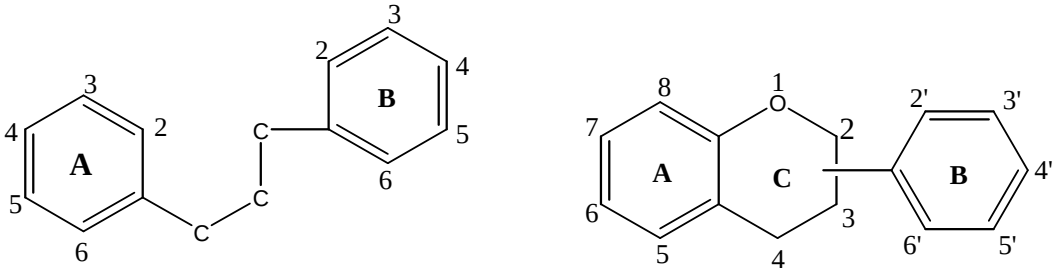

(A) **(B)**

Figure 3. The chemical structure of flavonoids based on a C_{15} skeleton can be represented as the C_6- C_3 - C_6 system (A). A CHROMANE ring bearing a second aromatic ring B in position 2, 3 or 4 (B).

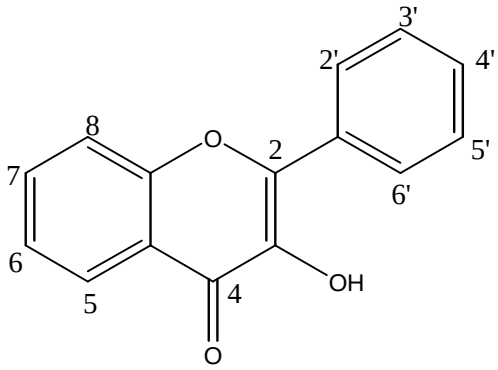

Flavonols

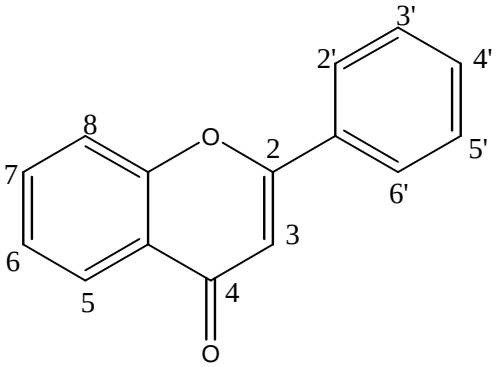

Flavons

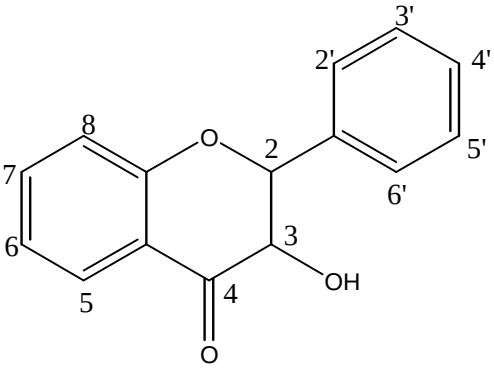

Flavanols

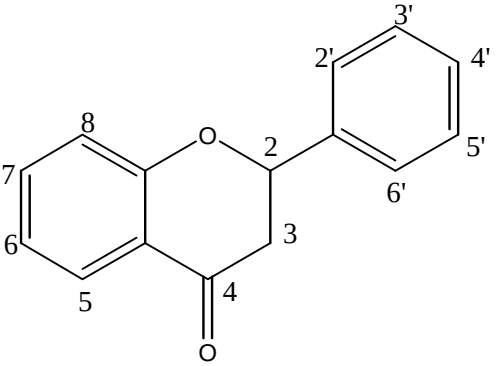

Flavanons

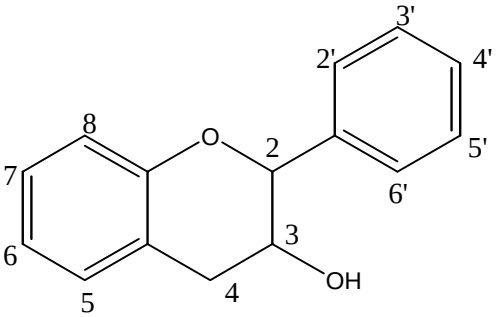

Anthocyanins

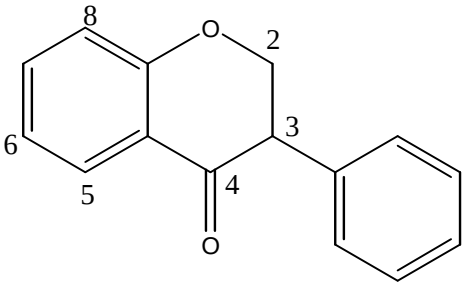

Isoflavonoids

Figure 4. Major subgroups of flavonoids.

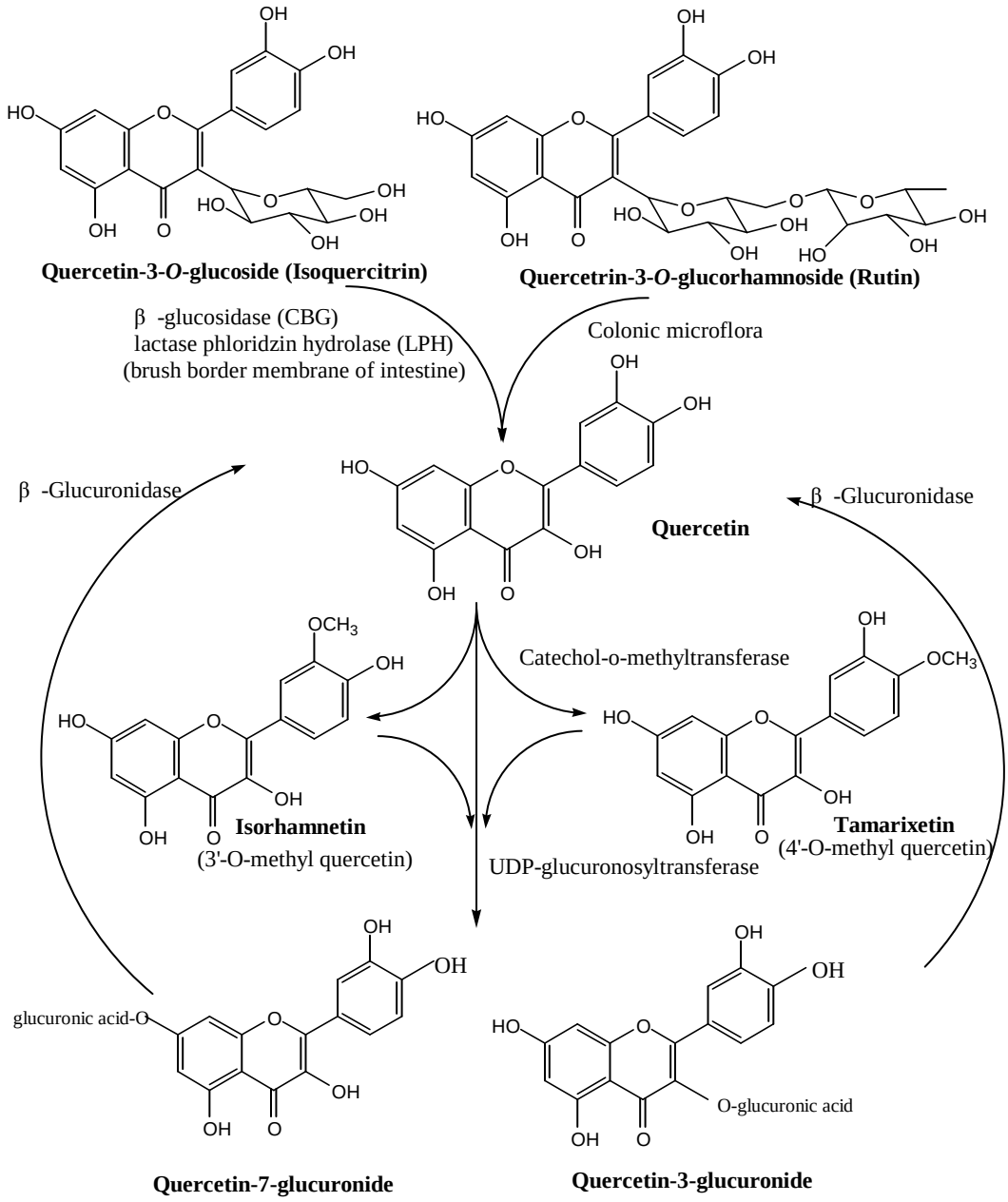

Figure 5. Biotransformation scheme of the nature quercetin (glucosides) via gastrointestinal system. (Structures of quercetin, isoquercitrin and rutin, and the methylated quercetin metabolites, isorhamnetin and tamarixetin).

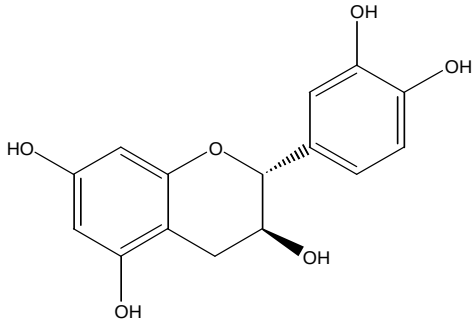

(+)-Catechin (C)

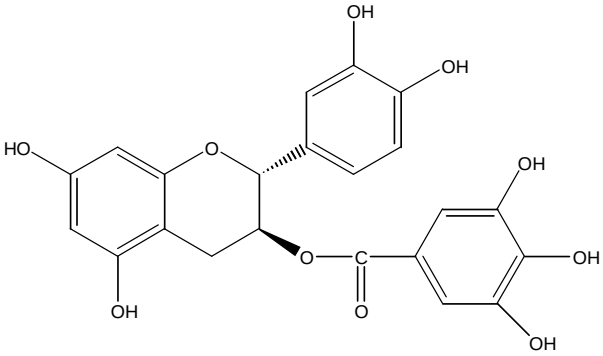

(-)-catechin gallate (CG)

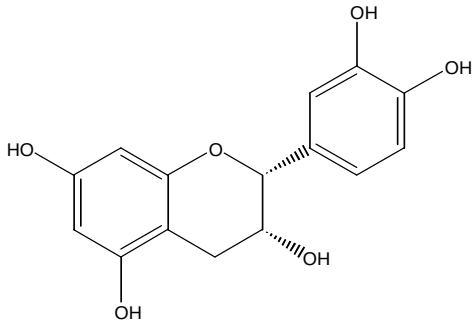

(-)-epicatechin (EC)

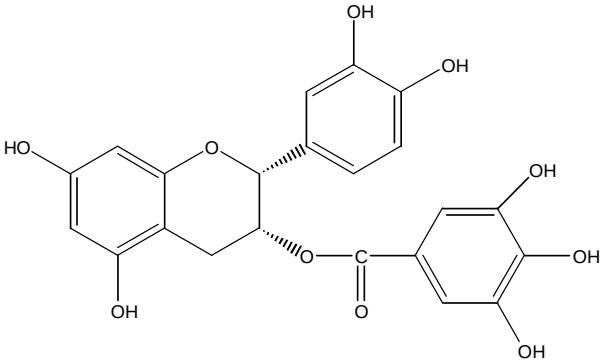

(-)-epicatechin gallate (ECG)

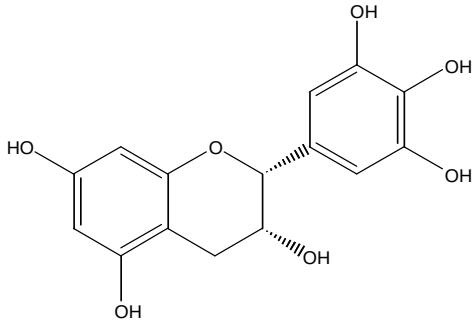

(-)-epigallocatechin (EGC)

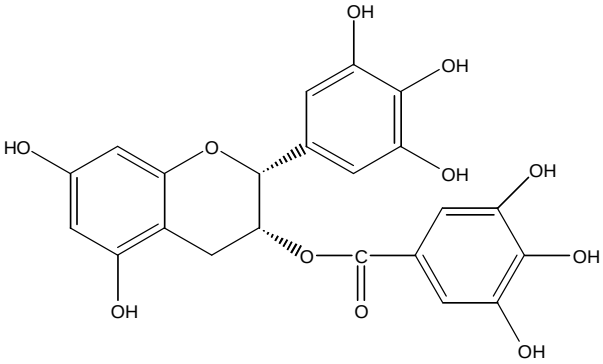

(-)-epigallocatechin gallate (EGCG)

Figure 6. Chemical structures of catechins.

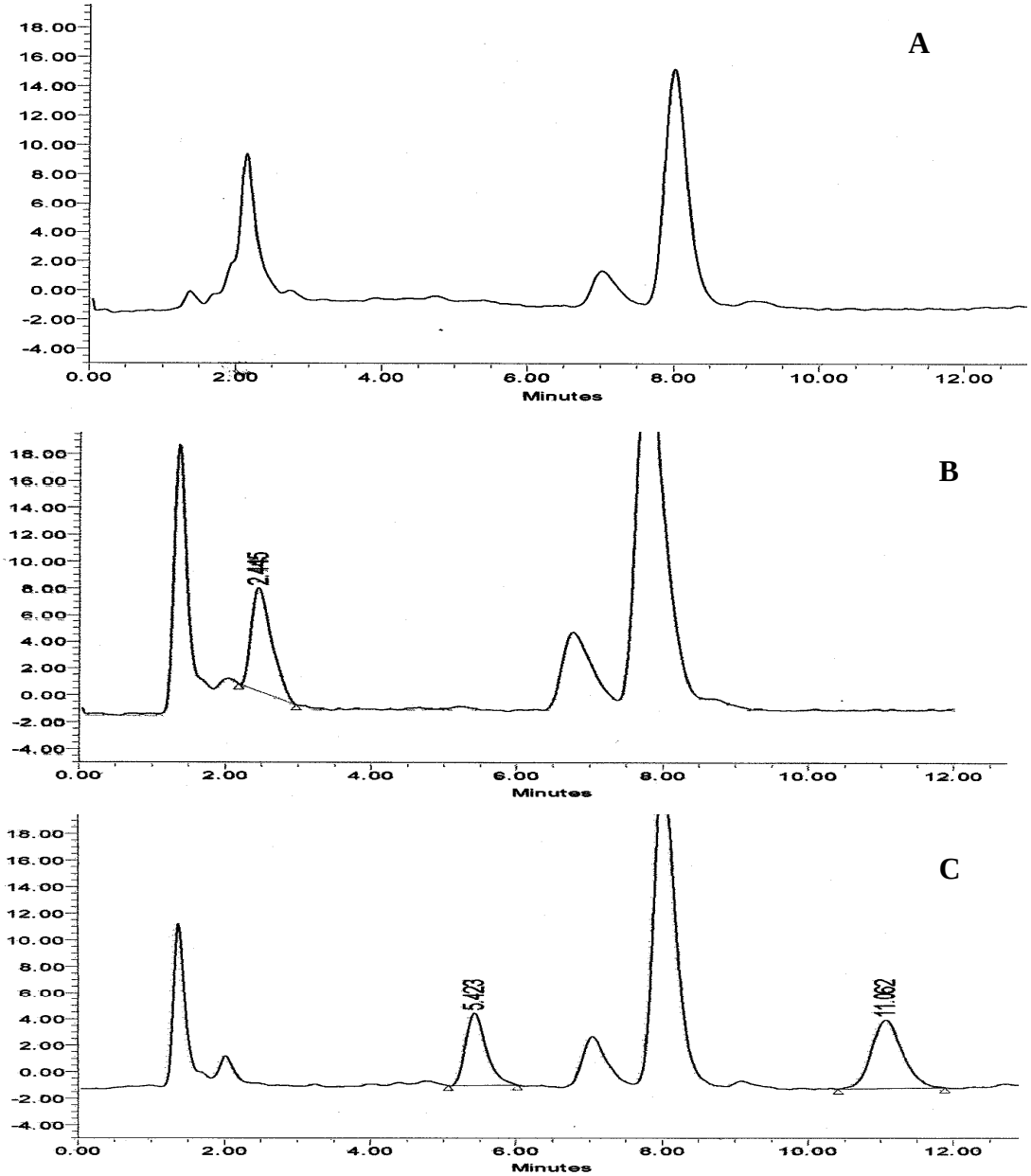

Figure 7. Chromatogram of blank rat plsma (A) and the plasma after oral adminstration of verapamil without etoposide adminstration (B, verapamil retention time 2.4 min), and the plasma 2 h after i.g. administration of etoposide at a dose of 10 mg/kg (C, podophyllotoxin at 5.4 min and etoposide at 11.1 min).

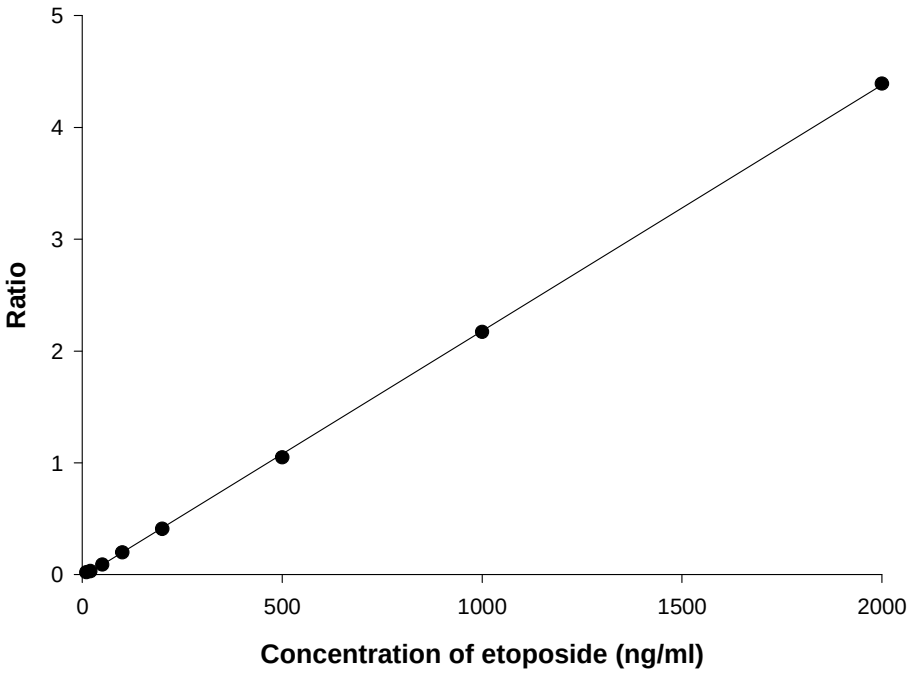

Figure 8. Calibration curve of etoposide when spiked in rat's blank plasma, where *y* is the peak area ratio of etoposide against podophyllotoxine and *x* is the concentration of etoposide, $y = 0.00215\,x - 0.00383$, $r^2 = 0.999$.

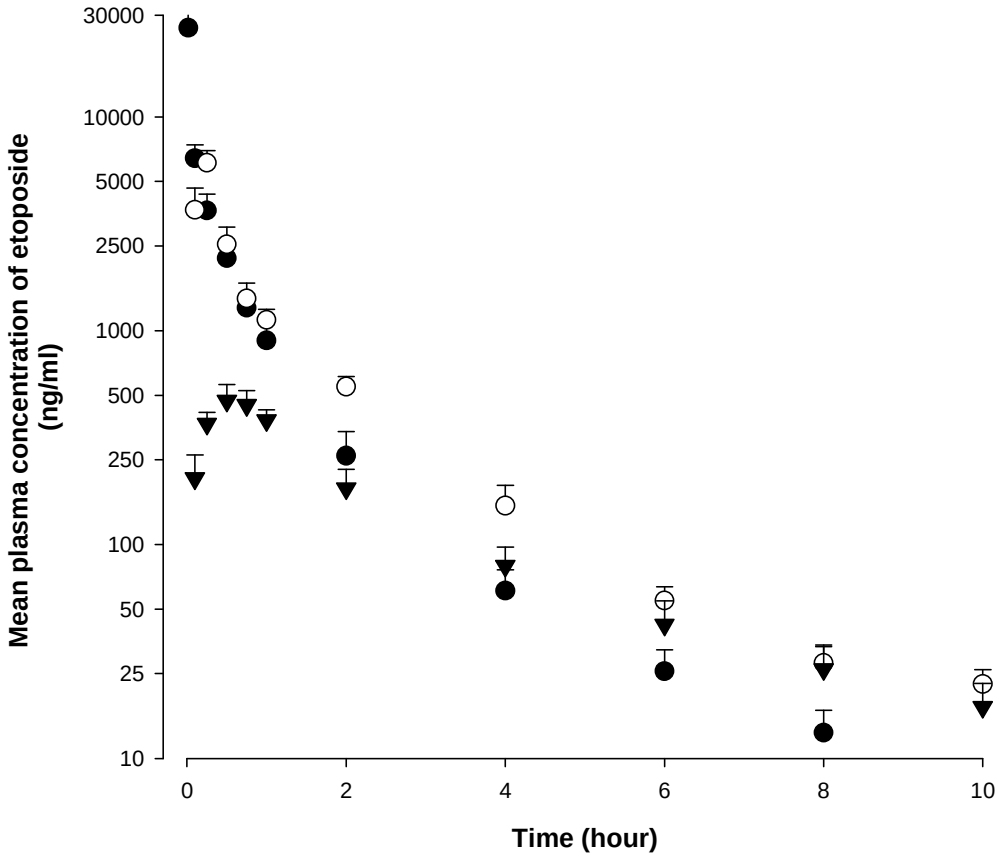

Figure 9. Mean plasma concentration-time profiles of etoposide after intravenous (3.3 mg/kg), intraportal (3.3 mg/kg) and intragastric (10 mg/kg) administration of etoposide to rats.

Bars represent the standard deviation (n = 6), (●), intravenous administration of etoposide at a dose of 3.3 mg/kg; (○), intraportal administration of etoposide at a dose of 3.3 mg/kg; (▼), intragastric administration of etoposide at a dose of 10 mg/kg.

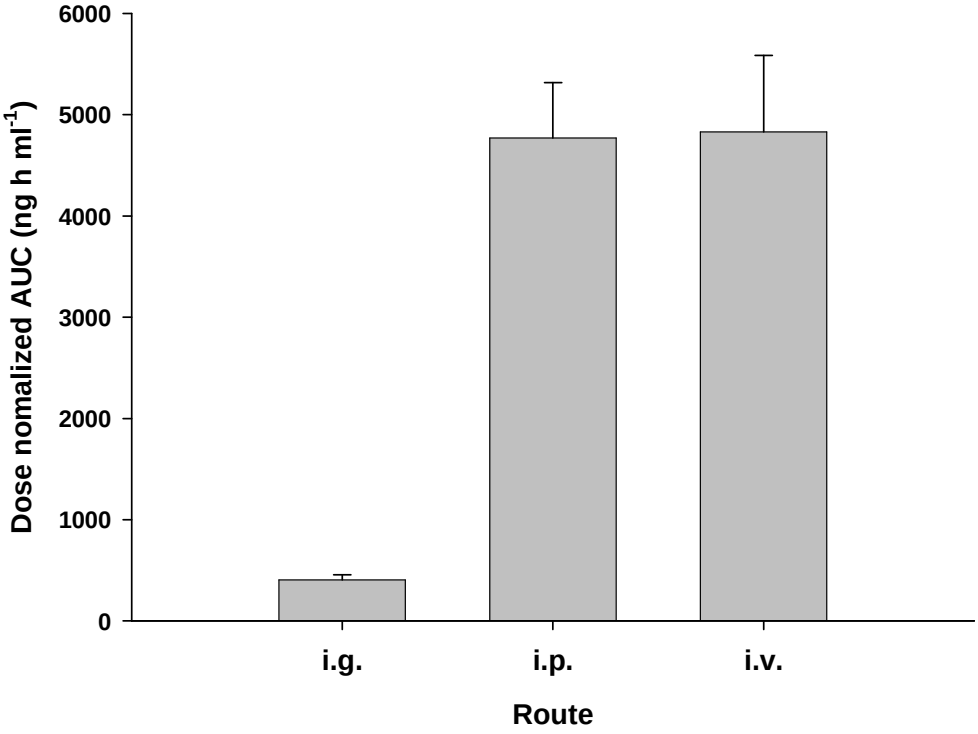

Figure 10. Mean dose-normalized (based on the dose of 3.3 mg/kg) $AUC_{0-\infty}$ values of etoposide following intravenous (i.v.), intraportal (i.p.) and intragastric (i.g.) administration to rats at a dose of 3.3, 3.3 or 10 mg/kg.

Bars represent the standard deviation (n = 6).

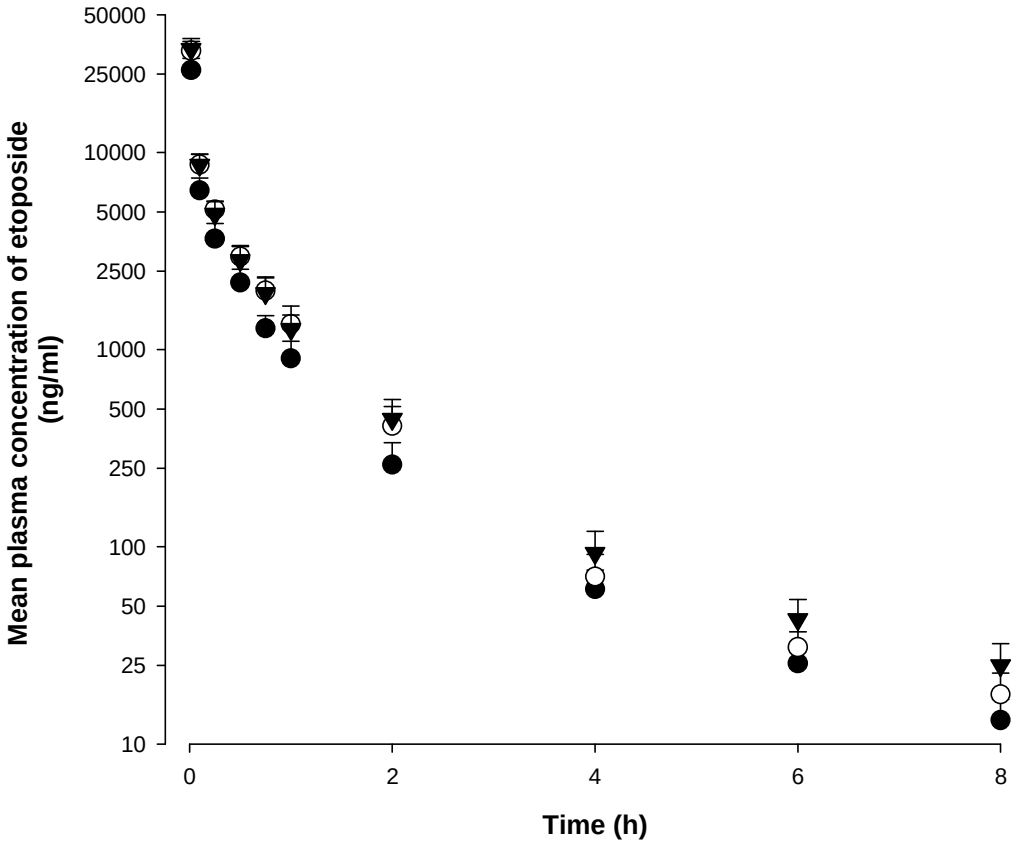

Figure 11. Mean plasma concentration-time profiles of etoposide after intravenous administration of etoposide at a dose of 3.3 mg/kg to rats in the presence or absence of verapamil at doses of 2 and 6 mg/kg (n = 6, each).

Bars represent the standard deviation. (●), intravenous administration of etoposide at a dose of 3.3mg/kg; (○), in the presence of 2 mg/kg of verapamil; (▼), in the presence of 6 mg/kg of verapamil.

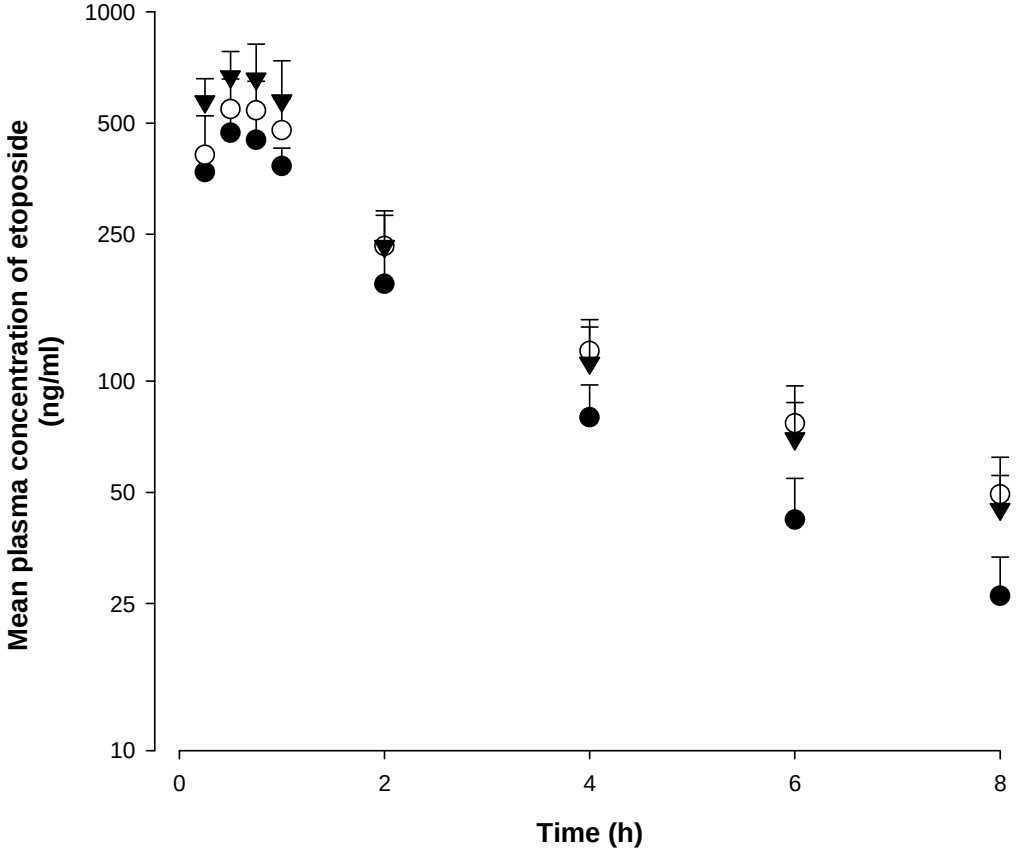

Figure 12. Mean plasma concentration-time profiles of etoposide after intragastric administration of etoposide at a dose of 10 mg/kg to rats in the presence or absence of verapamil at doses of 2 and 6 mg/kg (n = 6, each).

Bars represent the standard deviation. (●), intragastric administration of etopside at a dose of 10 mg/kg; (○), in the presence of 2 mg/kg of verapamil; (▼), in the presence of 6 mg/kg of verapamil.

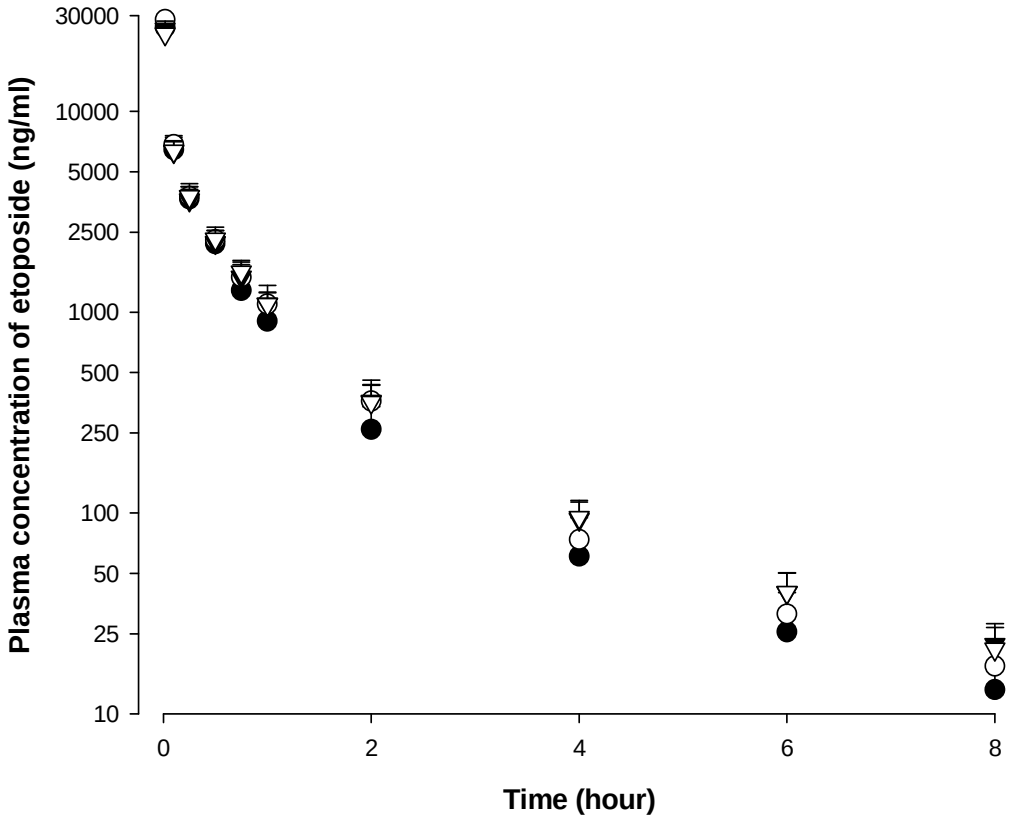

Figure 13. Mean plasma concentration-time profiles of etoposide after intravenous administration of etoposide at a dose of 3.3 mg/kg to rats in the presence or absence of quercetin at doses of 3, 12 and 20 mg/kg (n = 6, each).

Bars represent the standard deviation. (●), intravenous administration of etoposide at a dose of 3.3mg/kg; (○), in the presence of 3 mg/kg of quercetin; (▼), in the presence of 12 mg/kg of quercetin; (▽), in the presence of 20 mg/kg of quercetin.

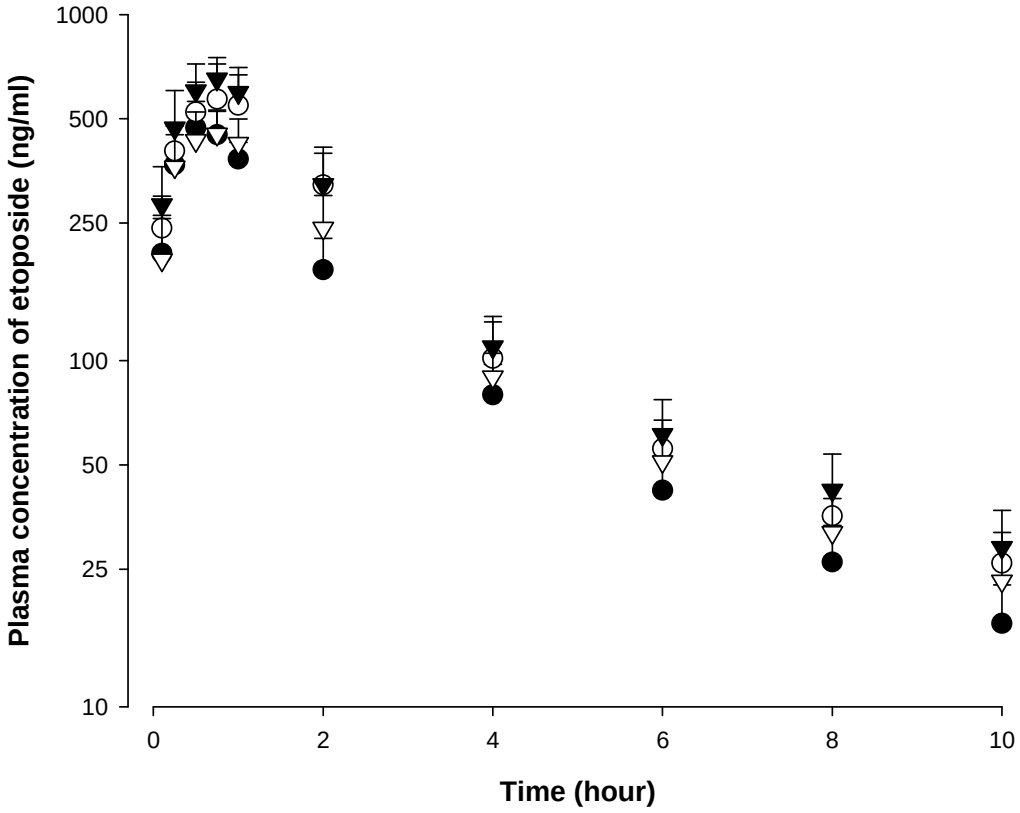

Figure 14. Mean plasma concentration-time curves of etoposide after oral administration of etoposide at a dose of 10 mg/kg to rats in the presence or absence of quercetin at doses of 3, 12 and 20 mg/kg (n = 6, each).

Bars represent the standard deviation. (●), intragastric administration of etopside at a dose of 10 mg/kg; (○), in the presence of 3 mg/kg of quercetin; (▼), in the presence of 12 mg/kg of quercetin; (▽), in the presence of 20 mg/kg of quercetin.

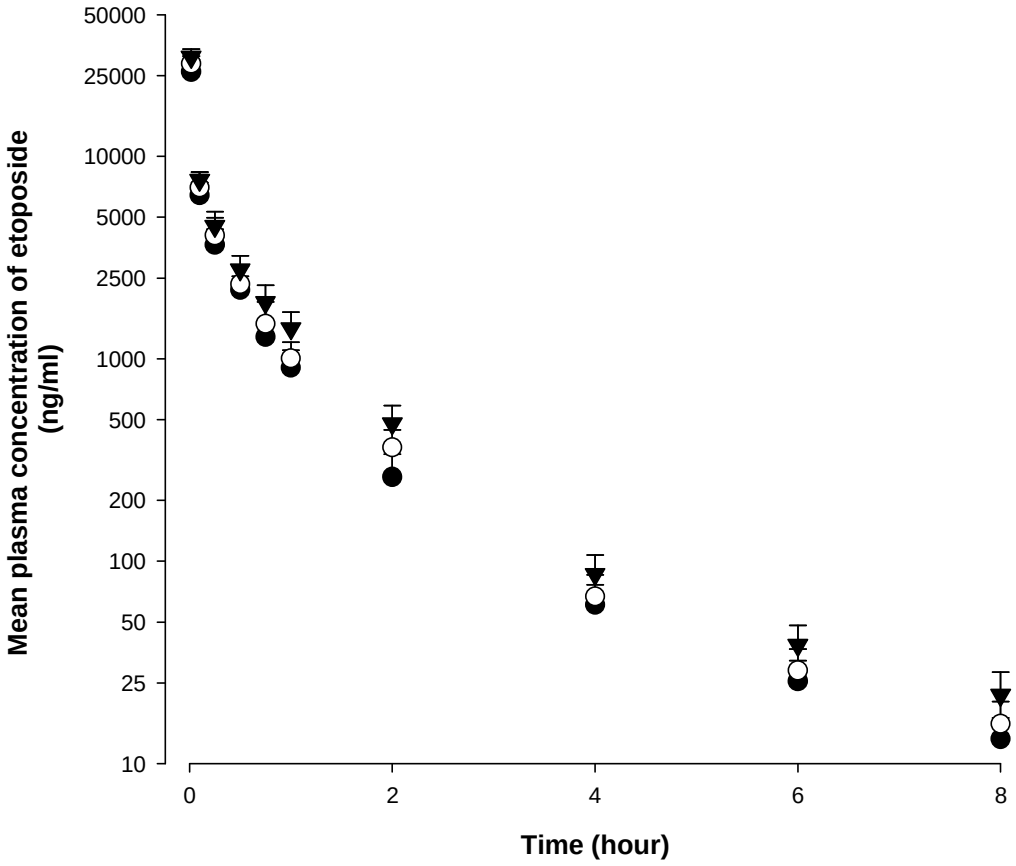

Figure 15. Mean plasma concentration-time profiles of etoposide after intravenous administration of etoposide at a dose of 3.3 mg/kg to rats in the presence or absence of EGCG at doses of 3 and 12 mg/kg (n = 6, each).

Bars represent the standard deviation. (●), intravenous administration of etoposide at a dose of 3.3 mg/kg; (○), in the presence of 3 mg/kg of EGCG; (▼) in the presence of 12 mg/kg of EGCG.

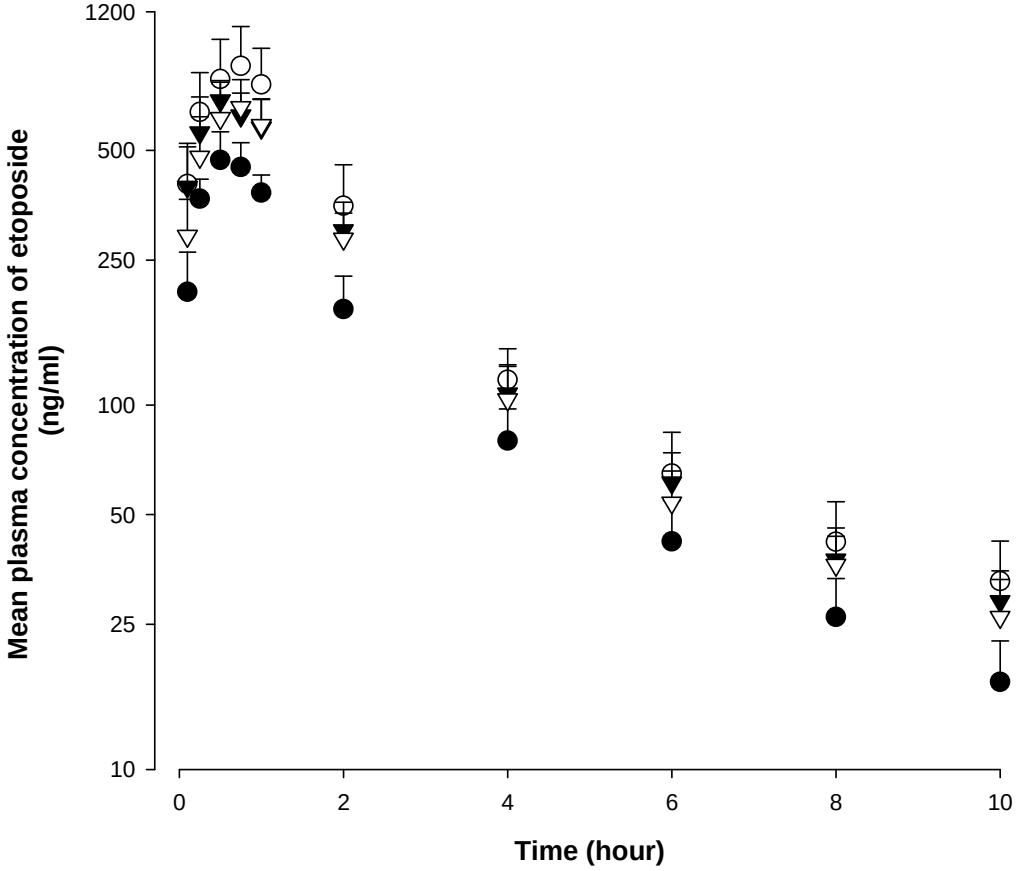

Figure 16. Mean plasma concentration-time curves of etoposide after intragastric administration of etoposide at a dose of 10 mg/kg to rats in the presence or absence of EGCG at doses of 3, 12 and 20 mg/kg (n = 6, each).

Bars represent the standard deviation. (●), intragastric administration of etopside at a dose of 10 mg/kg; (○), in the presence of 3 mg/kg of EGCG; (▼), in the presence of 12 mg/kg of EGCG; (▽), in the presence of 20 mg/kg of EGCG.

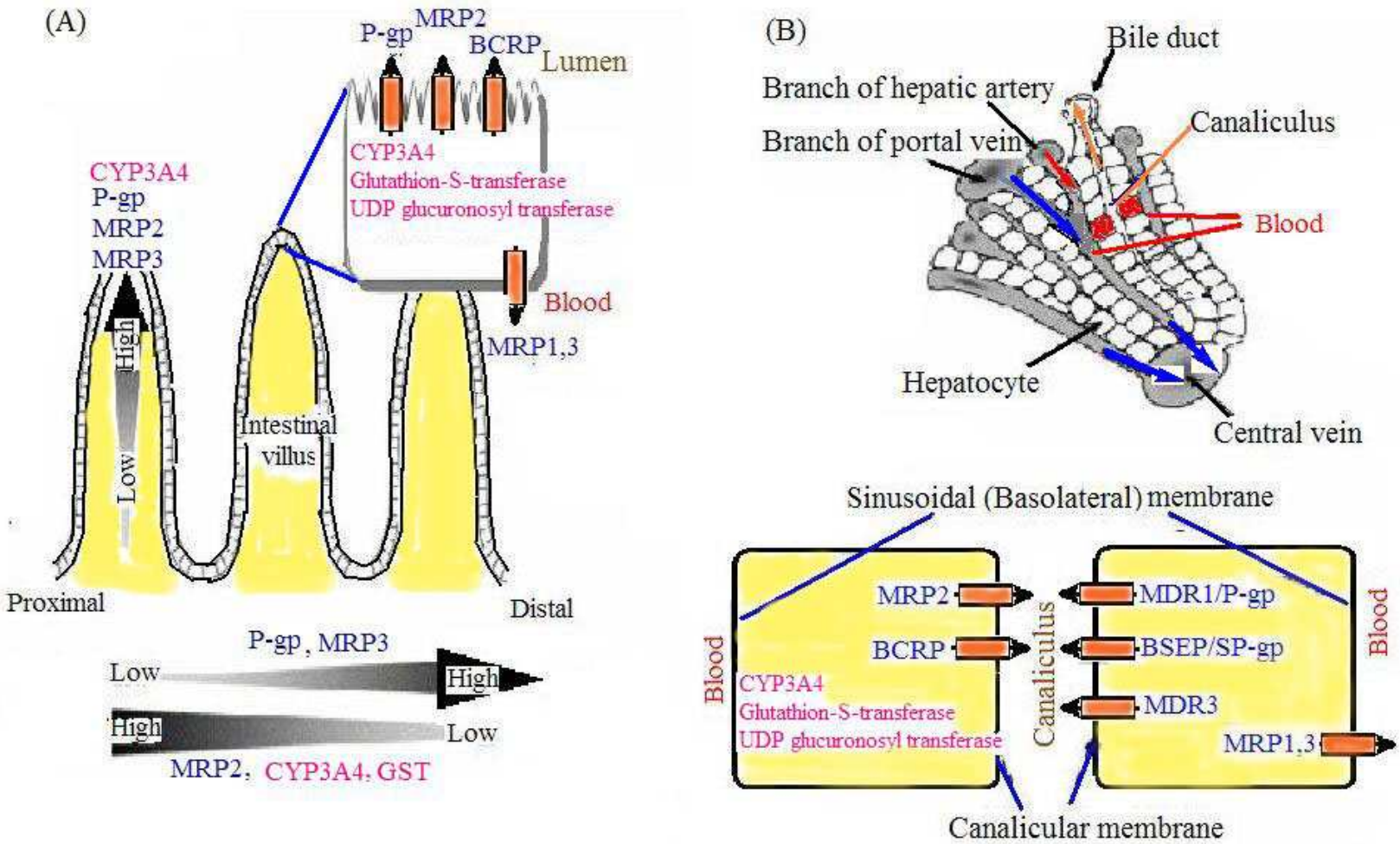

Figure 17. Efflux transporters and intracellular metabolic enzymes in intestinal epithelia (A) and hepatocytes (B).

Acknowledgements

I would like to express my gratitude to my advisor, Dr. Jun Shik Choi, for intitiating and encouraging me in the research of pharmacokinetics fields, and for the time he devoted and the precise way in which he has corrected and criticized the thesis and offered many helpful suggestions. The Thesis Committee Members, examiners, Professor Myung Gull Lee, Sang Chul Shin, Hoo Kyun Choi and Hyo Kyung Han to whom I extend my sincere thanks, gave me the excellent comments. I will not forget the help given by Professor Jin-Pil Burm who gave me many instructions and advices in grasping the experimental technology and statistics. I am luck to have a good laboratory collegue, Mr. Yong-Ji Piao, who had envariably made my thesis to be completed much easier. My gratitude also extends to Mr. Yong-Ri Qian for his kind support. Lastly, I have been fortunate in my wife, Xianglan Jin, my lovely son, Zhennan Li, given me much encouragement in my works.

저작물 이용 허락서

학 과	약학과	학 번	20047347	과 정	박사
성 명	한글 : 이수국 한문 : 李秀國 영문 : Xiuguo Li				
주 소	광주광역시 동구 서석동 375 번지 조선대학교 약학대학 약제학실				
연락처	E-mail : lishiuguo@hanmail.net				
논문제목	한글: 흰쥐에서 퀠세틴과 카테친이 에토포시드의 생체이용율에 미치는 영향 영문: The effect of quercetin and (-)-epigallocatechin gallate, on the bioavailability of etoposide in rats				

본인이 저작한 위의 저작물에 대하여 다음과 같은 조건아래 조선대학교가 저작물을 이용할 수 있도록 허락하고 동의합니다.

- 다 음 -

1. 저작물의 DB 구축 및 인터넷을 포함한 정보통신망에의 공개를 위한 저작물의 복제, 기억장치에의 저장, 전송 등을 허락함
2. 위의 목적을 위하여 필요한 범위 내에서의 편집・형식상의 변경을 허락함. 다만, 저작물의 내용변경은 금지함.
3. 배포・전송된 저작물의 영리적 목적을 위한 복제, 저장, 전송 등은 금지함.
4. 저작물에 대한 이용기간은 5 년으로 하고, 기간종료 3 개월 이내에 별도의 의사표시가 없을 경우에는 저작물의 이용기간을 계속 연장함.
5. 해당 저작물의 저작권을 타인에게 양도하거나 또는 출판을 허락을 하였을 경우에는 1 개월 이내에 대학에 이를 통보함.
6. 조선대학교는 저작물의 이용허락 이후 해당 저작물로 인하여 발생하는 타인에 의한 권리 침해에 대하여 일체의 법적 책임을 지지 않음
7. 소속대학의 협정기관에 저작물의 제공 및 인터넷 등 정보통신망을 이용한 저작물의 전송・출력을 허락함.

동의여부 : 동의 (√) 반대 ( )

2007 년 02 월

저작자: 이수국 (인)

조선대학교 총장 귀하